A Data-Driven Model of Waste Gasification and Pyrolysis: One Tailored Approach for an Experimental Facility from the Czech Republic

Dejan Brkić *, Pavel Praks, Judita Buchlovská Nagyová, Michal Běloch, Martin Marek, Jan Najser, Renáta Praksová, Jan Kielar

Posted Date: 18 December 2025

doi: 10.20944/preprints202512.1609.v1

Keywords: hydrogen; pyrolysis; symbolic regression; syngas; software; waste-to-energy

 doi:10.20944/preprints202512.1609.v1

Article

A Data-Driven Model of Waste Gasification and Pyrolysis: One Tailored Approach for an Experimental Facility from the Czech Republic

Dejan Brkić [1,2,*], **Pavel Praks** [1], **Judita Buchlovská Nagyová** [1], **Michal Běloch** [1], **Martin Marek** [3,4], **Jan Najser** [3], **Renáta Praksová** [1] **and Jan Kielar** [3]

[1] IT4Innovations, VSB – Technical University of Ostrava, Ostrava, Czech Republic
[2] Faculty of Electronic Engineering, University of Niš, Niš, Serbia
[3] ENET Centre, VSB – Technical University of Ostrava, Ostrava, Czech Republic
[4] Department of Technical Studies, College of Polytechnics Jihlava, Jihlava, Czech Republic
* Correspondence: dejan.brkic@elfak.ni.ac.rs

Abstract

The increasing demand for sustainable energy production necessitates the development of innovative technologies for converting municipal waste into valuable energy offering a viable alternative to fossil fuels. This study presents a flexible, portable, and expandable waste-to-energy concept that integrates gasification and pyrolysis processes production of combustible gases and liquid fuels. Particular emphasis is placed on the use of transparent and interpretable modeling approaches to support system optimization and future scalability. The proposed methodology is demonstrated on two experimental systems currently operated at CEET Explorer, VSB – Technical University of Ostrava, Czech Republic: (i) a primary gasification facility equipped with a plasma torch, reactor, hydrogen separator and tank, fuel cells, and renewable grid connections; and (ii) a secondary pyrolysis unit designed to maximize pyrolysis oil production. Both systems are modeled and simulated using in-house software developed in Python, employing stoichiometric balances, symbolic regression, and polynomial regression to represent chemical reactions and energy flows. The findings demonstrate that transparent models—such as stoichiometric modeling combined with interpretable machine learning—can accurately reproduce the operational behavior of waste-to-energy processes. Gasification is optimized for hydrogen generation and electricity production via fuel cells, whereas pyrolysis favors liquid fuel yield with syngas as a by-product. Molar mass relations are applied to ensure consistent conversion between mass and volume across gasification, pyrolysis, and combustion pathways, maintaining the conservation of mass. Overall, the integration of stoichiometric balance models with symbolic and polynomial regression provides a reliable and interpretable framework for simulating real waste-to-energy systems. The current results, based on bio-wood waste from the Czech Republic, validate the proposed methodology, which is made openly available to promote transparency, reproducibility, and further advancement of sustainable waste-to-energy technologies.

Keywords: hydrogen; pyrolysis; symbolic regression; syngas; software; waste-to-energy

1. Introduction

The objective of this study is to create flexible, portable, durable, ecologically sustainable, and expandable technology solution for efficient transformation of waste into valuable energy forms (taking care about, e.g., evidence that plasma gasification of municipal and/or industrial waste enables hydrogen production with superior environmental and thermodynamic performance when coupled with CO_2 capture [1], that catalytic pyrolysis of bio-waste enhances product yield and quality

 doi:10.20944/preprints202512.1609.v1

while reducing emissions [2], that pyrolysis and gasification of solid waste can be directed toward high-value outputs such as methanol, hydrogen, and electricity [3], etc.), especially in combustible gases obtained in gasification facility (primary facility) or in liquid fuel obtained in small pyrolysis facility (secondary facility, i.e. pyrolysis is auxiliary process).

Both systems are modeled and simulated using in-house software developed in Python, employing stoichiometric balances, symbolic regression, and polynomial regression to represent chemical reactions and energy flows. The interactive bilingual Python software is available at https://shinyenet.vsb.cz/. To foster transparency and ensure reproducibility of our research, we provide open-source codes, including an MS Excel tool that integrates key thermochemical processes of the Centre for Energy and Environmental Technologies – Explorer (CEETe, https://ceet.vsb.cz/en/CEETe/). The methodology is fully transparent and based on open-source resources, leveraging both regression and stoichiometric modeling. In addition, an automated reporting tool for gasification analysis is made available as open source. The tool is available as Electronic Appendix A. The present work focuses on technologies currently implemented at CEETe and complements the recent techno-economic analyses of energy supply systems (e.g., [4]). Unlike prior studies, all models introduced here are openly accessible in a public repository.

An Excel table that provides raw data sets from repeated gasification measurements to cover the uncertainty of measurements is given as Electronic Appendix B. The repository also includes a Python-based automated regression tool for gasification modeling and reporting, provided as Electronic Appendix C.

1.1. Background

A rough schema of facilities and processes in the observed waste-to-energy system is given in Figure 1.

Main products in the facilities examined are:

1. Primary facility: Gas mixture from gasification, i.e., syngas, which is mainly composed of nitrogen N_2, hydrogen H_2, carbon monoxide CO, carbon dioxide CO_2, and methane CH_4, depends on the type of waste and gasification temperature.

2. Secondary facility: Pyrolysis oil (liquid fuel) is the main product from pyrolysis.

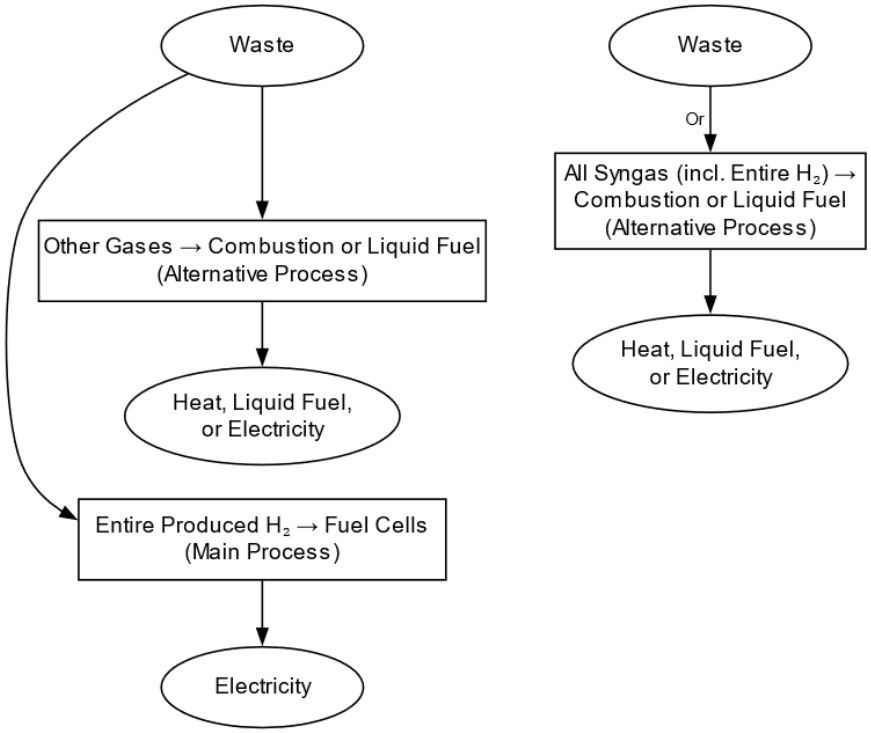

 doi:10.20944/preprints202512.1609.v1

(a) Gasification

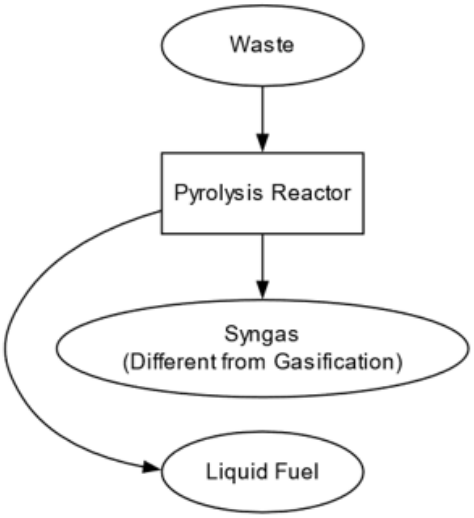

(b) Small-Scale Pyrolysis

Figure 1. Schematic representation of facilities and processes in the observed waste-to-energy system: (a) Gasification, (b) Small-scale pyrolysis. In the gasification process, additional hydrogen may be supplied by an electrolyzer as part of an auxiliary system.

The gasification facility (primary facility) includes a plasma torch, gasification reactor, and fuel cell unit for producing hydrogen in a main process (e.g., Aziz et al. [5] review thermochemical and biological routes for converting biomass and organic waste to hydrogen, highlighting recent progress, key technologies, and challenges for advancing a sustainable hydrogen economy), with auxiliary process for producing hydrogen in an electrolyzer. Combustion for heating (or conventional electricity generation via a turbine), or the production of liquid fuel, is used as an alternative process. This alternative process operates only when the fuel cells in the main process are turned off, or in parallel with other available gases—mainly methane and carbon monoxide, in addition to hydrogen. The entire amount of produced hydrogen is used either in the main process or in the alternative process. Other non-combustible gases are envisaged for the possible production of liquid fuel after chemical treatment. Small pyrolysis is a separate facility (secondary facility).

1.2. Literature Overview

Synthetic gases had been frequently used before the Second World War, but were later substituted with natural gas due to environmental issues. These issues have since been overcome by using cleaner technologies and by substituting the type of alternative fuel (raw material for both examined facilities), i.e. to switch from coal to communal waste. For example, dos Santos et al. [6] find that a natural gas–based hydrogen industry with CO_2 capture can aid the energy transition but depends on oil prices and CO_2 storage capacity. Thomas [7] shows that the manufactured gas industry transformed lighting and safety, expanded to energy and chemicals, and became the first integrated energy network before natural gas replaced it. Melaina [8] shows that the manufactured gas industry, once central to urban lighting and heating, illustrates how innovation, competition, and adaptability shaped energy networks, offering lessons for today's hydrogen infrastructure. Wehrer [9] reviews how legacy manufactured gas plant sites still threaten groundwater with toxic organic and inorganic contaminants, highlighting knowledge gaps in pollutant behavior and the need for improved risk assessment and remediation. Hamper [10] reviews the history of U.S. manufactured gas plants, their decline with the rise of natural gas and electricity, and details how different

 doi:10.20944/preprints202512.1609.v1

production processes generated distinct gases and residuals, knowledge essential for assessing former plant sites. Albertazzi et al. [11] highlight biomass gasification as a renewable, CO_2-neutral energy source and explore challenges in reforming high-sulfur and alkali-rich gas streams for liquid fuel production. Liebs [12] gives an overview about town gas), e.g., different carbon footprint is for hydrogen production from coal, from waste, from water, or from hydrocarbons. Maksimov et al. [13] analyze water use and carbon footprints in hydrogen production, showing that nearly half of the hydrogen from steam reforming originates from water with lower emissions, highlighting water and energy balances as key factors for sustainable hydrogen development. Also, pyrolysis was not always popular because it can form unwanted and toxic hydrocarbons if the process is not controlled with care. For example, Lyu et [14] al. show that biochars produced at higher pyrolysis temperatures (>400°C) are less toxic and have lower dioxin-like potencies, making them more suitable as soil adsorbents, and Rutkowski and Lewin [15] show that thermal decomposition of certain plastics produces toxic gases, mainly carbon monoxide and hydrogen cyanide, with hazards comparable to other common polymers.

Syngas (gases from gasification or as byproduct of pyrolysis) is different compared to natural gas in which hydrocarbons and especially methane is dominant. Among others, Rahimpour et al. [16] give an extensive overview about syngas production, and Odel [17] overviews facts relating to the production and substitution of manufactured gas for natural gas). Hydrogen from syngas can be used for blending with natural gas as demonstrated in Erdener et al. [18], who examine the potential of blending hydrogen into natural gas grids, highlighting technical, safety, and regulatory challenges while identifying research gaps for wider integration, and in Ozturk et al. [19], who show that blending hydrogen with natural gas improves combustion efficiency and reduces CO_2 and CO emissions, though NOx trends fluctuate and some environmental impacts slightly increase. Composition of syngas from pyrolysis is very different from that of syngas from gasification.

This article is organized into two main parts, namely modeling and description of in-house developed software based on developed models which can be used for various testing. A data-driven digital model of waste gasification and pyrolysis includes machine learning methods [20-23]. Ascher et al. [20] apply machine learning to model biomass and waste gasification, showing gradient boosting as most accurate and demonstrating that interpretability methods improve trust and insights for process design. Li et al. [21] use machine learning to model biomass gasification, showing gradient boosting predicts product yields accurately and identifies optimal feed and temperature conditions for maximizing H_2-rich syngas. Lee et al. develop an Artificial Neural Network (ANN)-based model for steam methane reforming using extensive operational data, achieving high prediction accuracy and optimizing process conditions to reach 85.6% thermal efficiency. Chu et al. develop regression and neural network models to predict syngas characteristics in plasma gasification of municipal waste, showing key roles of input power, feedstock, and gas flow rates in determining efficiency and composition.

Waste is alternative fuel used instead of fossil fuels, while hydrogen is used here as energy source as a predominant alternative for fossil fuels as presented in Kaheel et al. [24], who review the hydrogen energy landscape, identifying technical, policy, logistical, and infrastructure challenges affecting production, distribution, and deployment of hydrogen energy, and underscores the importance of public–private partnerships, regulation, and strategic planning to accelerate blue and green hydrogen adoption globally.

2. Waste-to-Energy Experimental Facilities — Models of the System

Gasification and pyrolysis are two complementary thermochemical conversion routes for valorizing waste and low-rank fuels. Gasification, particularly in co-gasification setups, has shown strong potential to address global waste challenges while enhancing hydrogen-rich syngas production and process efficiency [25]. Plastic waste, for example, is increasingly recognized as an energy resource, with co-gasification improving gas yield, cold gas efficiency, and fuel quality compared to single-feed processes [26]. Similarly, blending low-rank coals with refuse-derived fuels

 doi:10.20944/preprints202512.1609.v1

has been demonstrated as a feasible strategy to produce hydrogen-rich syngas and improve feedstock usability [27]. Pyrolysis, on the other hand, enables the thermal decomposition of plastics and biomass into liquid fuels, syngas, and char, thereby complementing gasification in integrated waste-to-energy and resource recovery systems.

The main difference between pyrolysis (a secondary facility) and gasification (a primary facility) is that pyrolysis takes place without access to oxygenators, while gasification takes place in presence of ambient air.

The temperature in both examined facilities is set [28] in order to:

1. maximize hydrogen production from syngas from gasification [29], i.e., from the primary facility for use in fuel cells (main process in the primary facility); alternatively, if fuel cells are out of order, the goal is to maximize the energy value of syngas for combustion and heating purposes (alternative process of the primary facility),

2. maximize the production of liquid fuel (pyrolysis oil) [30-32], which is the main optimization goal to achieve in pyrolysis, i.e., in the secondary facility.

Gasification (primary facility) takes place in a reactor with a temperature ranging from 750 °C to 1100 °C, while pyrolysis from 300 °C to 800 °C.

2.1. Gasification Facility – Primary Facility of the Observed Waste-to-Energy System

The gasification is the primary facility in the examined waste-to-energy system, with a diagram given in Figure 2.

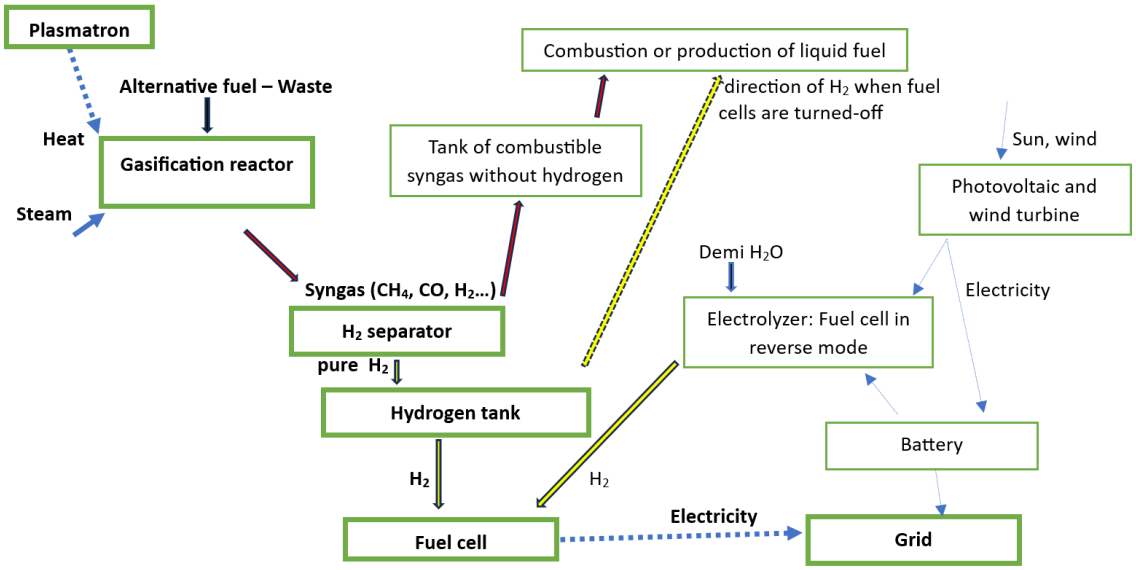

Figure 2. Syngas production and utilization in the gasification facility as the primary waste-to-energy unit. Bold green boxes and bold text denote the main process involving hydrogen-to-electricity conversion in fuel cells.

Air is used as the gasification medium in the gasification facility. Fuel (alternative fuel) for the system is waste, mostly municipal waste, which consists mainly of organic materials (biomass or combustibles from communal garbage and industry). It is used to produce synthetic gas – syngas. The main process within the facility goes through a hydrogen separator and tank [33] and fuel cells to produce electricity from hydrogen. It is connected to a battery, electric grid with integrated photovoltaic and wind turbine [34]. An electrolyzer which can produce hydrogen from water through electrolysis, is also part of the system as a support to the main process as an auxiliary process. In addition, a combustion unit (with an envisaged alternative to produce liquid fuel through Fischer-Tropsch synthesis) is added to the gasification system as an alternative process, which operates only when the main process is turned off (i.e., when fuel cells are turned off), and vice versa. For the

 doi:10.20944/preprints202512.1609.v1

moment, the entire amount of hydrogen produced goes entirely or in the main process or in alternative process. Alternatively, combustion as a variant of the alternative process can work without hydrogen only with methane and carbon monoxide in parallel with the main process. Combustion can be replaced with the production of liquid fuel where non-combustible compounds of syngas possibly can be used.

Gasification is characterized by the following parameters: Fuel cells with the installed capacity of 40kW (with 5 stacks of 8 kW), an electrolyzer 14 kW, battery with capacity of 500 kWh with an inverter of 250 kVA, connections to photovoltaic with the capacity of up to 170 kW, and wind power up to 10 kW. Waste is used as an alternative fuel with an input of 60-80 kg/hour with calorific values of 21.1 and 27.12 MJ/kg where the energy required for the separation of H_2 from syngas is missing, for example, biomass) [35]. The energy required for compression from 1 to 200 bars at a flow rate of 0.39 kg/h is about 11.98 kWh if the efficiency of the compressor is 50%.

The input/output relations within the processes of the gasification facility are identified in Table 1.

Table 1. Process input–output relations in the primary gasification facility.

[a] **Main process**	Input	Output
Plasmatron	Nozzle base constant k [dimensionless] Plasma torch power P [kW] Filling pressure of air f_p [bar]	Middle plasma torch temperature T [K]
Gasification reactor	Alternative fuel – Waste Heat [c] (Middle plasma temperature T [K] transformed to temperature in the gasification reactor t [°C]) Steam, i.e., water	Syngas Waste residual
Hydrogen separator	Syngas	Pure hydrogen Syngas without hydrogen
Hydrogen tank	Hydrogen from Hydrogen separator	Hydrogen
Fuel cells	Hydrogen from Gasification Hydrogen from Electrolyzer	[d] Electricity
Auxiliary process	Input	Output
Electrolyzer	Electricity (from Battery or Photovoltaics/Wind turbine) Water (Demi water)	Hydrogen
[b] Alternative process	Input	Output

 doi:10.20944/preprints202512.1609.v1

Tank of combustible syngas without hydrogen	Syngas without hydrogen	Combustible syngas without hydrogen Non-combustible compounds of syngas
Combustion	Combustible syngas without hydrogen Hydrogen	Heat
Production of liquid fuel	Combustible syngas without hydrogen Non-combustible components of syngas Hydrogen	Liquid fuel

[a] bold letters signify/indicate the main process within the gasification facility; [b] when the main process operates, then the alternative process does not operate and vice versa; while combustion can alternatively work in parallel with methane and carbon monoxide; [c] only because the available raw parameters these values of temperature are expressed in different units: T[K] vs. t [°C]; [d] Grid, battery, photovoltaics, and wind turbine

The components of the gasification facility, such as Alternative fuel, Gasification reactor, Plasma torch, Hydrogen separation and tank, Fuel cells, Electrolyzer, Combustion or production of liquid fuel, Photovoltaics, and wind turbine, will be explored in more detail in the following text.

Input of waste for gasification is estimated to 20 kg per hour, which can give around 17.6-18.33 normal m^3 of syngas (or for 100 kg of waste it can give around 88 normal cubic meters of syngas; initially about 150 normal m^3 of syngas were estimated for 100 kg of waste production; however, it was extremely ambitious, knowing that mass of waste plus reactants from ambient air need to be equal to the mass of the produced syngas) while further details are given in Table 2.

Table 2. Waste-to-energy conversion estimates in the gasification facility for an amount of 20 kg of waste at the process temperature of 930°C.

Gas compound	normal m^3	Number of mol	Mass of gas [kg]	Mass %	Composition Vol. %
H_2	≈ 3.5	154.5	≈ 0.3	≈ 1.5	19.7
CO_2	≈ 2	88.9	≈ 3.9	≈ 19.5	11.3
CO	≈ 3.7	163.4	≈ 4.6	≈ 22.8	20.8
CH_4	≈ 0.4	17.5	≈ 0.3	≈ 1.4	2.2
N_2	≈ 8.8	393.4	≈ 11	≈ 54.8	50.1
Σ	≈ 18.3	818.0	≈ 20	100	104.1

* Volume of 1 mol of ideal gas is 0.0224 normal cubic meters at T=273.15 K and p=101325 Pa

 doi:10.20944/preprints202512.1609.v1

Based on Boyle's law (Boyle–Mariotte law), Charles' law, and Gay-Lussac's law, pV=nRT, where p is pressure in Pa, V is volume in cubic meters, n is number of mol, T is temperature in K, and the universal gas constant is R=8.3144598 $m^3 \cdot Pa/(mol \cdot K)$. The following can be concluded, as given in Table 3.

Table 3. Amount of Produced Gas for Various Process Parameters in Gasification Facility.

Gas compound	Number of mol n	nR [$m^3 \cdot Pa/K$]	known T [K]	Known V [m^3]	p [bar]
H_2	154.5	1284.9	50	5	≈ 0.13
CO_2	88.9	739.8	50	5	≈ 0.07
CO	163.4	1359.3	50	5	≈ 0.14
CH_4	17.5	145.7	50	5	≈ 0.01
N_2	393.4	3271.3	50	5	≈ 0.33
Σ	818.0	6801.2	50	5	≈ 0.68
[a] Gas compound	Number of mol	nR [$m^3 \cdot Pa/K$]	known p [bar]	Known V [m^3]	T [K]
H_2	154.5	1284.9	41.5	5	16176.8
CO_2	88.9	739.8	37.3	5	25244.7
CO	163.4	1359.3	138.1	5	50801.3
CH_4	17.5	145.7	19.6	5	67237.1
N_2	393.4	3271.3	202.7	5	30985.7
Σ	818.0	6801.2	439.3	5	32301.0
[a] Gas compound	Number of mol	nR [$m^3 \cdot Pa/K$]	known p [bar]	known T [K]	V [m^3]
H_2	154.5	1284.9	41.5	50	≈ 0.015
CO_2	88.9	739.8	37.3	50	≈ 0.010
CO	163.4	1359.3	138.1	50	≈ 0.005
CH_4	17.5	145.7	19.6	50	≈ 0.004
N_2	393.4	3271.3	202.7	50	≈ 0.008
Σ	818.0	6801.2	439.3	50	≈ 0.008

[a] first three columns are repeated from above

2.1.1. Alternative Fuel

 doi:10.20944/preprints202512.1609.v1

Fuel for gasification and pyrolysis should be communal waste or combustible residuals from industry and biomass (Figure 3). The waste is mechanically preprepared before being sent to the gasification reactor.

Figure 3. Prepared Waste Serving as an Alternative Fuel for Gasification.

2.1.2. Plasma Torch

A plasma torch enables gasification of municipal waste in the gasifier reactor [36]. A plasma torch is a device for generating a stream of plasma with an appropriate temperature [37]. In this case, the middle plasma torch temperature T [K], which depends on the required power of plasma torch P [kW], the base constant of nozzle k [dimensionless], and the filling pressure f_p [bar], is given in Equation (1):

$$T = 700 + \frac{19050 \cdot P}{k \cdot f_p} \quad (1)$$

The plasma torch from this study provides low-temperature plasma with a middle plasma torch temperature T ranging from min. 1295.3K to max. 19750.0K based on real physical experiments [38-41]. Equation (1), based on symbolic regression [38], gives very accurate predictions only in this range, where it is well correlated with experimental data with the relative error that remains below 0.283‰ (0.0283%) [42].

2.1.3. Gasification Reactor - Amount and Composition of Syngas Based on Temperature

Gasification is performed in a reactor in the presence of air while heat is provided by the low-temperature plasma torch. In the model, the composition of syngas depends on the temperature in the gas reactor from Equation (1) as given in Table 4. The gasification facility with the reactor in its core is given in Figure 4.

 doi:10.20944/preprints202512.1609.v1

Figure 4. Gasification facility with the reactor at the core of the process.

Waste gasification is performed in a reactor with temperature t ranging from 750 °C to 1100 °C in the presence of air that is used as the gasification medium. The plasma torch, which is used for this study, provides plasma with a middle plasma torch temperature T ranging from min. 1295 K to max. 19750 K based on real physical experiments which further should be reduced to the required temperature prescribed for the gasification reactor as given in Equation (2):

$$t=(T-273.15)\cdot 0.01917+726.59 \quad (2)$$

Where t is the middle temperature in the gasification reactor in [°C], and T is the temperature of the plasma torch in [K] as seen in Equation (1). The values of the temperature are expressed in different units—T [K] vs. t [°C]—solely because of the available structure's raw parameters from the available datasets. An additional reference for the syngas composition for comparisons is Hasanzadeh et al. [43], where the composition of syngas in air gasification is reported: H_2≈18%, CO≈15%, CH_4≈3-4%, CO_2≈10%, and N_2≈60%. While in steam gasification it is as follows: H_2≈62%, CO≈21%, CO_2≈3-4%, and CH_4≈1-2%.

Table 4. Syngas composition dependence on temperature

	Gas compound in vol. %				
Temperature t [°C] in gasification reactor	CO_2	H_2	CO	CH_4	N_2
750	8.1	9.7	29.4	4.4	45.2
800	9.8	10.9	26.0	4.0	46.2

 doi:10.20944/preprints202512.1609.v1

900	11.9	16.0	20.1	2.2	48.4
1000	11.3	12.8	19.9	1.7	52.8
1050	11.5	12.3	18.8	1.2	55.0
1100	12.3	11.8	12.4	1.0	56.3

The composition of syngas depends mostly on the temperature in the gasification reactor, oxidation medium, and the composition of waste, while the most desired component is hydrogen because the main purpose of the facility is to produce electrical energy from hydrogen in fuel cells. The desired components of syngas are also methane and carbon monoxide, which can be further used for direct combustion (for heating or for the production of electricity) or for the production of liquid fuels through Fisher-Tropsch synthesis [44, 45]. Carbon dioxide can also be used for carbon production [46].

Gasification is simulated using two types of regression, symbolic and polynomial (based on a similar analysis as in [47], polynomial formulations can be recommended for use in this case[1]). Symbolic regression is a technique based on artificial intelligence with the ability to explore appropriate mathematical expressions for identifying the best-fit models for a given dataset [48].

Based on data from Table 4 and using regression, both symbolic and polynomial, continual functions of five gases with largest volumetric percentage in syngas in dependence of temperature t [°C] in the gasification reactor are established (these five gases give in sum around 100%).

Symbolic regression functions for gasification are developed using the open-source tools AI Feynman [49]—previously applied in gasification modeling [50]—and PySR (High-Performance Symbolic Regression in Python and Julia) [51], alongside polynomial expressions. The resulting formulas are presented in Table 5.

Table 5. Regression Relations Between Middle Reactor Temperature (t [°C]) and Syngas Composition[a.]

Gas compound in % vol.	Model - Formula where t [°C] is the middle temperature in the gasification reactor
Polynomial regression 5 degree – Used in the final version of the developed waste-to-energy software	
H_2	$8.64427756 \times 10^{2} - 1.11535475 \times 10^{-2}\, t^{2} + 2.50417715 \times 10^{-5} t^{3} - 2.08318518 \times 10^{-8} t^{4} + 6.0929057 \times 10^{-12} t^{5}$
CO_2	$7.88262261 \times 10^{1} - 1.42644743 \times 10^{-3}\, t^{2} + 3.66824063 \times 10^{-6} t^{3} - 3.38728167 \times 10^{-9} t^{4} + 1.07816591 \times 10^{-12} t^{5}$
CO	$-7.75058073 \times 10^{2} + 1.12213487 \times 10^{-2}\, t^{2} - 2.59664968 \times 10^{-5} t^{3} + 2.22417149 \times 10^{-8} t^{4} - 6.70159810 \times 10^{-12} t^{5}$
CH_4	$-1.35270631 \times 10^{2} + 1.76696155 \times 10^{-3}\, t^{2} - 3.88540841 \times 10^{-6} t^{3} + 3.15797384 \times 10^{-9} t^{4} - 9.02717242 \times 10^{-13} t^{5}$
N_2	$-1.92588105 \times 10^{2} + 3.07852112 \times 10^{-3}\, t^{2} - 6.98410588 \times 10^{-6} t^{3} + 5.91052625 \times 10^{-9} t^{4} - 1.75956783 \times 10^{-12} t^{5}$

[1] Extended analysis is given in Appendix A

 doi:10.20944/preprints202512.1609.v1

Symbolic regression: Models obtained in PySR – Used in the final version of the developed waste-to-energy software	
H_2	=LN(ABS(0.000677729241918855×t^2×ABS(LN(ABS(0.0010822109×t)+0.00000001))^(-2.6401255))+0.00000001)
CO_2	=LN(ABS(-0.060511474×t^2+44.81684×t)+0.00000001)+2.0503674
CO	=0.7548879×t/(0.07978012×t-40.459797)
CH_4	=ABS(3.6089828-3679.8438/(t-300.00784))
N_2	=ABS(0.000001013×t-0.0017925174)^(-0.5535527)
Symbolic regression: AI Feynman with oscillatory tendencies [50] – Rejected for use after reanalysis	
H_2	1/(0.112277210469×COS(COS(((EXP(SIN((t+1)))-1)-1))))
CO_2	Model 1: 0.003263060755×(t×LN((SQRT(t)+SIN(LN(t))))) Model 2: TAN(-29.286471691464+SQRT((((t×EXP(COS((LN(t)+1))))-1)))
CO	6.719797422959×EXP(EXP(SIN(((((COS(t)-1))^(-1)+1))))
CH_4	(0.946772291789×(EXP(COS((EXP(SIN((t+t)))+1)))+1))^2
N_2	SQRT(-664.727896959755×((((COS(EXP(COS(t)))-1)-1)-1)-1))
Used in the evaluation in Appendix A of this article	
Model 1 CO_2	$\mathrm{logm}_{10}(t\, e^{\sin(t+0.6718609)})^2,\ \mathrm{logm}_{10} = \ln(\lvert t\rvert + 10^{-8})$
Model 2 CO_2	$\mathrm{logm}(-0.060511474\, t^2) + 2.0503674,\ \mathrm{logm} = \ln(\lvert t\rvert + 10^{-8})$
Model 1 H_2	$\frac{8.9065269419}{\cos(\cos(e^{\sin(t+1)} - 2))}$
Model 2 H_2	$\mathrm{logm}_2\left(7.744805\left(-9.837645 + \mathrm{logm}(t)\right)^{-1.5165994}\right) + 0.0054770974\, t,$ $\mathrm{logm}_2 = \log_2(\lvert t\rvert + 10^{-8})$
Model 3 H_2	$6.5368786 + \mathrm{logm}_2(\lvert -9.864973 + \mathrm{logm}_2(t)\rvert^{-2.1570945}),$ $\mathrm{logm}_2 = \log_2(\lvert t\rvert + 10^{-8})$
Model 4 H_2	Repeated model for H_2 from above in this Table from polynomial regression 5 degree

[a] polynomial models maintain the conservation of syngas volume better compared to symbolic models

The maximum production of hydrogen is around 900 °C in the reactor, while the temperature of the plasma torch is around T=10887.2 K. The goal is to maximize the production of hydrogen for further use in fuel cells. It is discovered after entropy analysis through Occam's Razor [47] that the results obtained in the AI Feynman software from [50] are not stabile, i.e., these symbolic regression formulas show oscillatory behavior between the points given in Table 4 as shown in Figure 5. In Figure 5a, the red line presents expected behavior, while in Figure 5b, the green line presents

 doi:10.20944/preprints202512.1609.v1

oscillatory behavior between the black dots. In both Figures 5a and 5b, these black dots represent real data from Table 4.

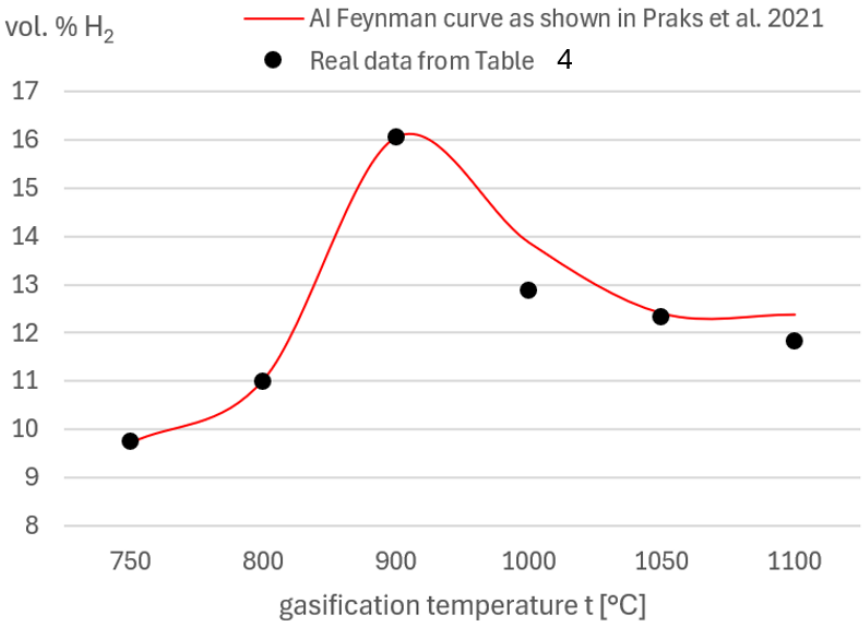

(a)

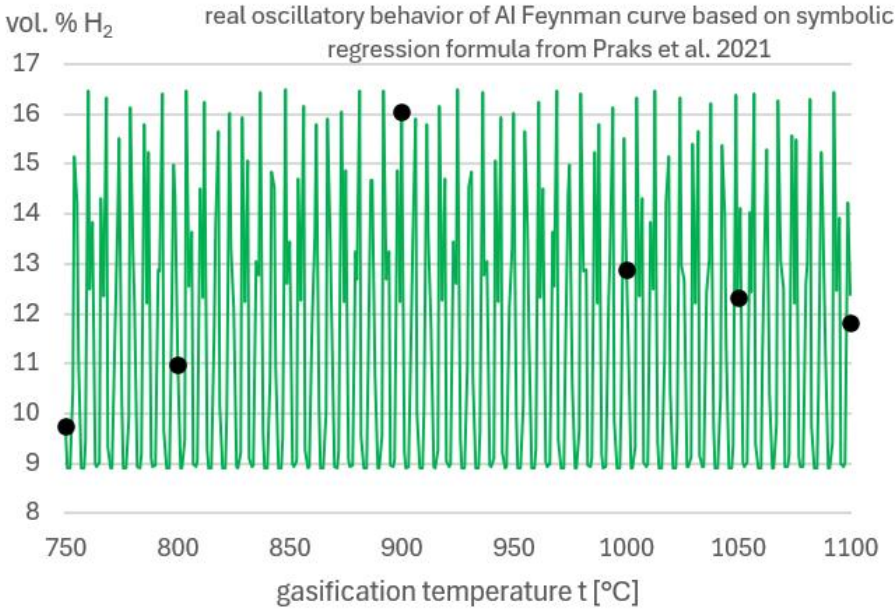

(b)

Figure 5. Hydrogen volumetric percentage vs. gasification temperature t [°C] (Black dots: experimental data from Table 4). (a) Red line: expected trend without intermediate values. (b) Green curve: oscillatory behavior from symbolic regression formulas as given in Praks et al., 2021 [50] and here in Table 5.

Suitable formulas for volumetric percentages are given in Figures 6 and 7.

According to the symbolic regression models obtained in PySR, for t=928 °C, an unrealistic peak for hydrogen occurs which is not confirmed in practice. An unreliable amount of hydrogen is predicted by PySR between 897°C and 955°C. However, this peak does not appear in polynomial

 doi:10.20944/preprints202512.1609.v1

regression models, where the sum of the entire amount of the produced syngas always remains below 100 %, as can be seen in Figure 8. Therefore polynomial models maintain the conservation of syngas volume better compared to symbolic models.

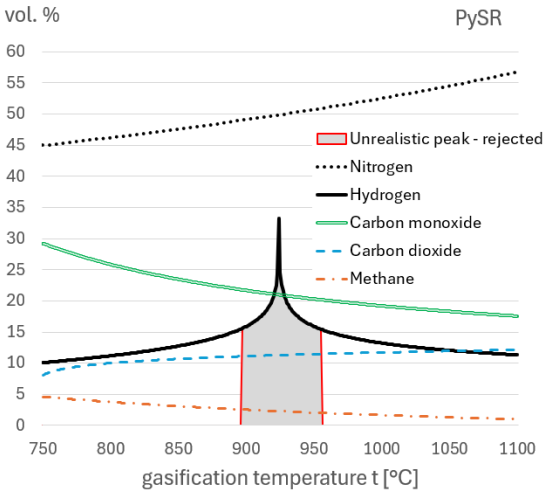

Figure 6. PySR-derived symbolic regression models for hydrogen, carbon dioxide, carbon monoxide, methane, and nitrogen (Table 5); volumetric percentage vs. gasification temperature t [°C].

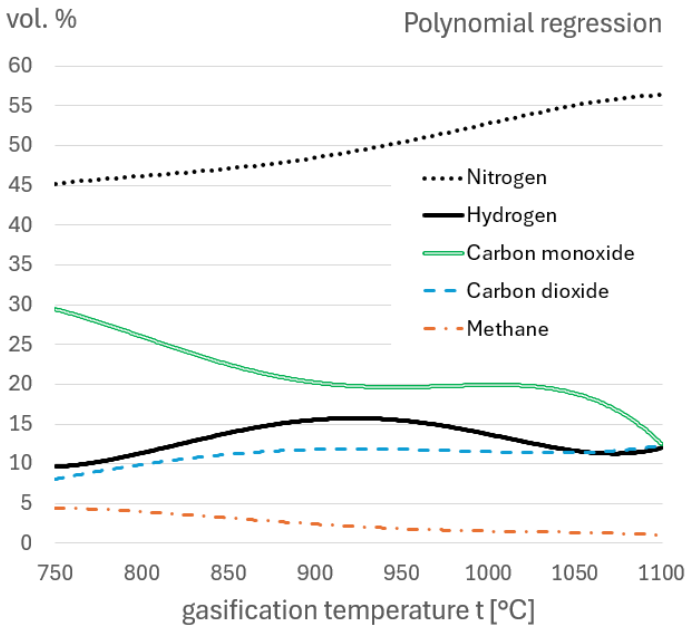

Figure 7. Polynomial regression models for hydrogen, carbon dioxide, carbon monoxide, methane, and nitrogen (Table 5); volumetric percentage vs. gasification temperature t [°C].

 doi:10.20944/preprints202512.1609.v1

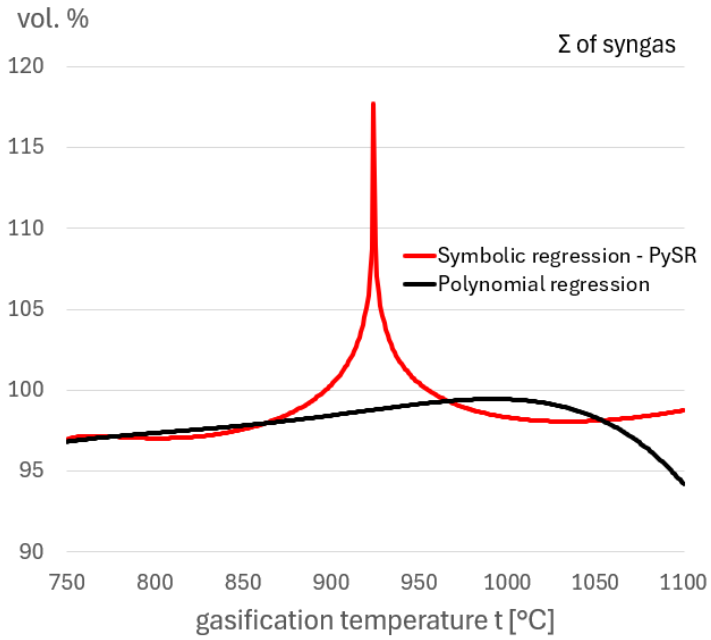

Figure 8. Sum of all syngas components: discrepancy >100% with PySR, while polynomial model yields a sum <100%; volumetric percentage vs. gasification temperature t [°C].

Models obtained in symbolic regression – PySR and polynomial regression can be combined with the exception hydrogen, for which only polynomial regression model should be used. In more detail:

- Polynomial regression: For the middle temperature in the gasification reactor t ranging from 879 °C and 966 °C, the production of hydrogen is maximal with an amount larger than 15% and never reaches 16%. The absolute peak for the production of H_2 is for t=923 °C. For t=923 °C, CO_2 11.87 %, CO 19.76 %, CH_4 2.11 %, and N_2 49.3 %, which gives a total of 98.78 % while the rest are other gases.
- Symbolic regression – PySR: A model for all components of syngas can be used except for hydrogen, for which polynomial regression formulation should be used instead.

Polynomial regression models perform better than symbolic regression models as confirmed by statistical and entropy analyses grounded in Occam's Razor [47]. Therefore, the polynomial regression approach will be further developed in more detail:

- **Hydrogen H_2**

The recommended model for hydrogen H_2 is a polynomial of degree 4, as given in Table 6. Its mean squared error is as low as 0.3.

Table 6. Optimized polynomial formulations between middle reactor temperature (t [°C]) and the amount of produced hydrogen H_2.

Polynomial degree	Hydrogen H_2
2	$-1.369\times 10^{-4}\ t^2+0.258\ t-106{,}612$

 doi:10.20944/preprints202512.1609.v1

3	$4.358\times 10^{-7}\, t^3-0.001\, t^2+1.372\, t-444.415$
4	$7.734\times 10^{-9}\, t^4-2.828\times 10^{-5}\, t^3+0.038\, t^2-22.876t+5070.377$
5	$6.251\times 10^{-12}\, t^5-2.139\times 10^{-8}\, t^4+2.573\times 10^{-5}\, t^3-0.011t^2-2.718\times 10^{-5}\, t+890.767$
6	$5.077\times 10^{-15}\, t^6-1.661\times 10^{-11}\, t^5+1.865\times 10^{-8}\, t^4-7.344\times 10^{-6}\, t^3-2.149\times 10^{-8}\, t^2+4.614\times 10^{-11}\, t+246.526$

Figure 9 shows optimized models of volumetric percentage of H_2 in dependence on temperature t [°C] in the gasification reactor obtained in polynomial regression.

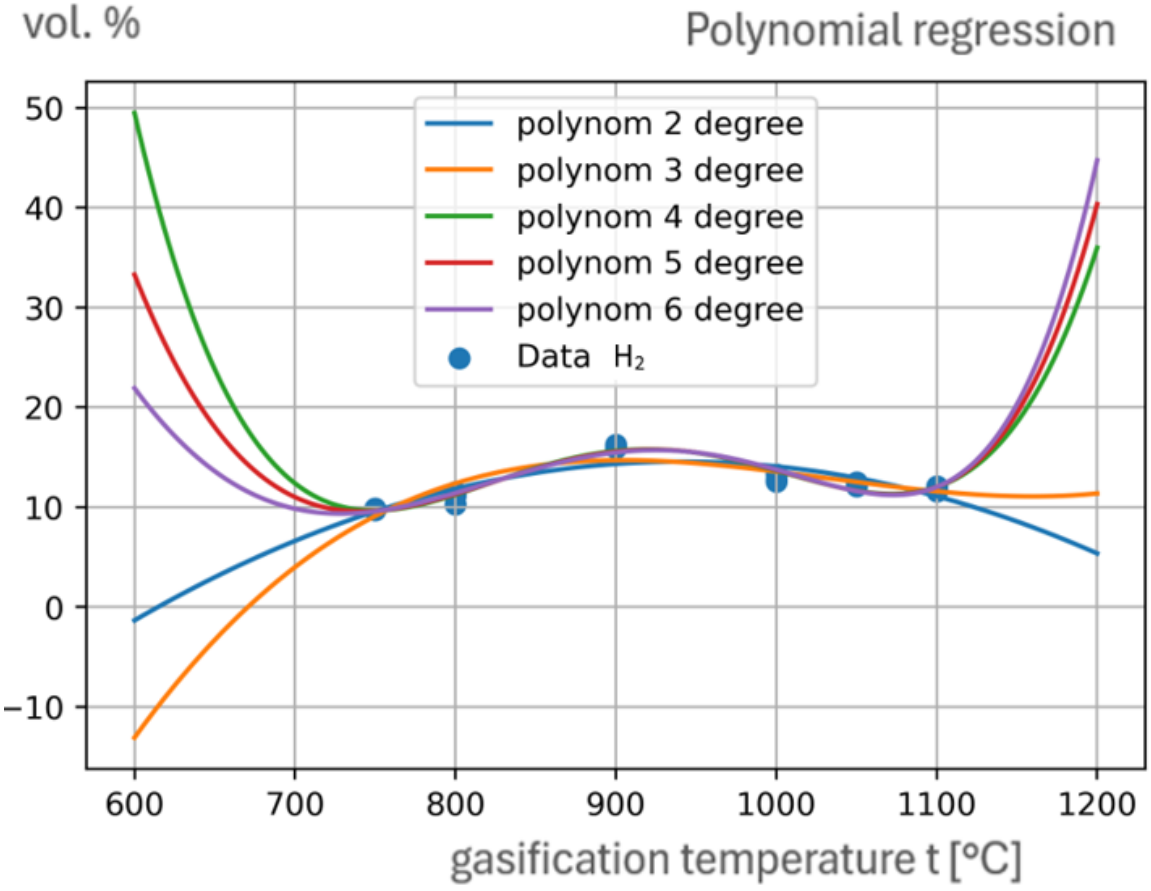

Figure 9. Volumetric percentage of hydrogen in the gasification reactor: Polynomial regression models valid for 750–1100 °C; volumetric percentage vs. gasification temperature t [°C]

- **Carbon dioxide CO_2**

The recommended model for carbon dioxide CO_2 is a polynomial of degree 4, as given in Table 7. Its mean squared error is as low as 0.4.

Table 7. Optimized polynomial formulations between middle reactor temperature (t [°C]) and the amount of produced carbon dioxide CO_2

Polynomial degree	Carbon dioxide CO_2

 doi:10.20944/preprints202512.1609.v1

2	$-4.67\times10^{-5}\,t^2+0.096t-37.252$
3	$4.215\times10^{-7}\,t^3-0.001t^2+1.173t-363.929$
4	$1.824\times10^{-9}\,t^4-6.35\times10^{-6}\,t^3+0.008t^2-4.545t+936.676$
5	$1.237\times10^{-12}\,t^5-3.945\times10^{-9}\,t^4+4.359\times10^{-6}\,t^3-0.002t^2-4.136\times10^{-6}\,t+105.442$
6	$7.534\times10^{-16}\,t^6-2.177\times10^{-12}\,t^5+2.071\times10^{-9}\,t^4-6.422\times10^{-7}\,t^3-1.88\times10^{-9}\,t^2+4.034\times10^{-12}\,t+6.226$

Figure 10 shows optimized models of volumetric percentage of CO_2 in dependence on temperature t [°C] in the gasification reactor obtained in polynomial regression.

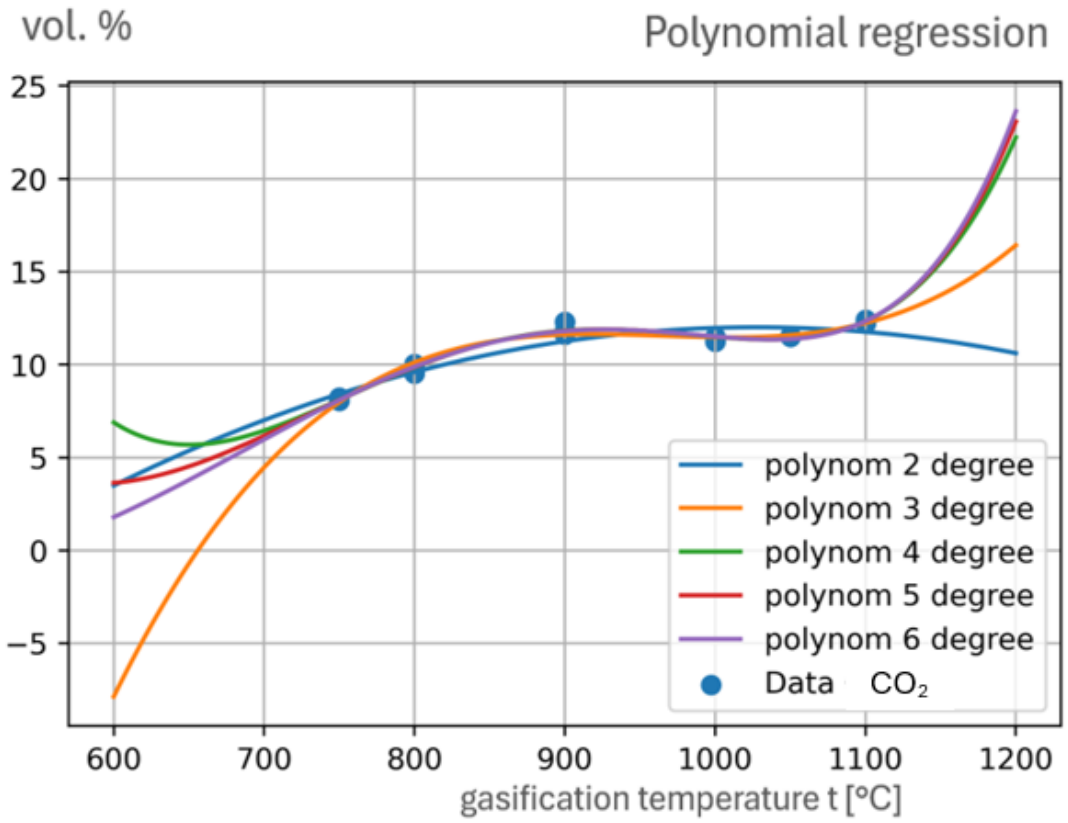

Figure 10. Volumetric percentage of CO_2 in the gasification reactor: Polynomial regression models valid for 750–1100 °C; volumetric percentage vs. gasification temperature t [°C].

- **Carbon monoxide CO**

The recommended model for carbon monoxide CO is a polynomial of degree 4, as given in Table 8. Its mean squared error is as low as 0.21.

Table 8. Optimized polynomial formulations between middle reactor temperature (t [°C]) and the amount of produced carbon monoxide CO.

Polynomial degree	Carbon monoxide CO

 doi:10.20944/preprints202512.1609.v1

2	$1.017\times10^{-4}t^2-0.219t+136.345$
3	$-5.873\times10^{-7}\,t^3+0.002t^2-1.721t+591.542$
4	$-3.807\times10^{-9}\,t^4+1.355\times10^{-5}\,t^3-0.018t^2+10.215t-2123.132$
5	$-2.742\times10^{-12}\,t^5+9.024\times10^{-9}\,t^4-1.036\times10^{-5}\,t^3+0.004t^2+1.029\times10^{-5}\,t-248.532$
6	$-1.85\times10^{-15}\,t^6+5.672\times10^{-12}\,t^5-5.85\times10^{-9}\,t^4+2.048\times10^{-6}\,t^3+5.995\times10^{-9}\,t^2-1.287\times10^{-11}\,t-0.241$

Figure 11 shows optimized models of volumetric percentage of CO in dependence on temperature t [°C] in the gasification reactor obtained in polynomial regression.

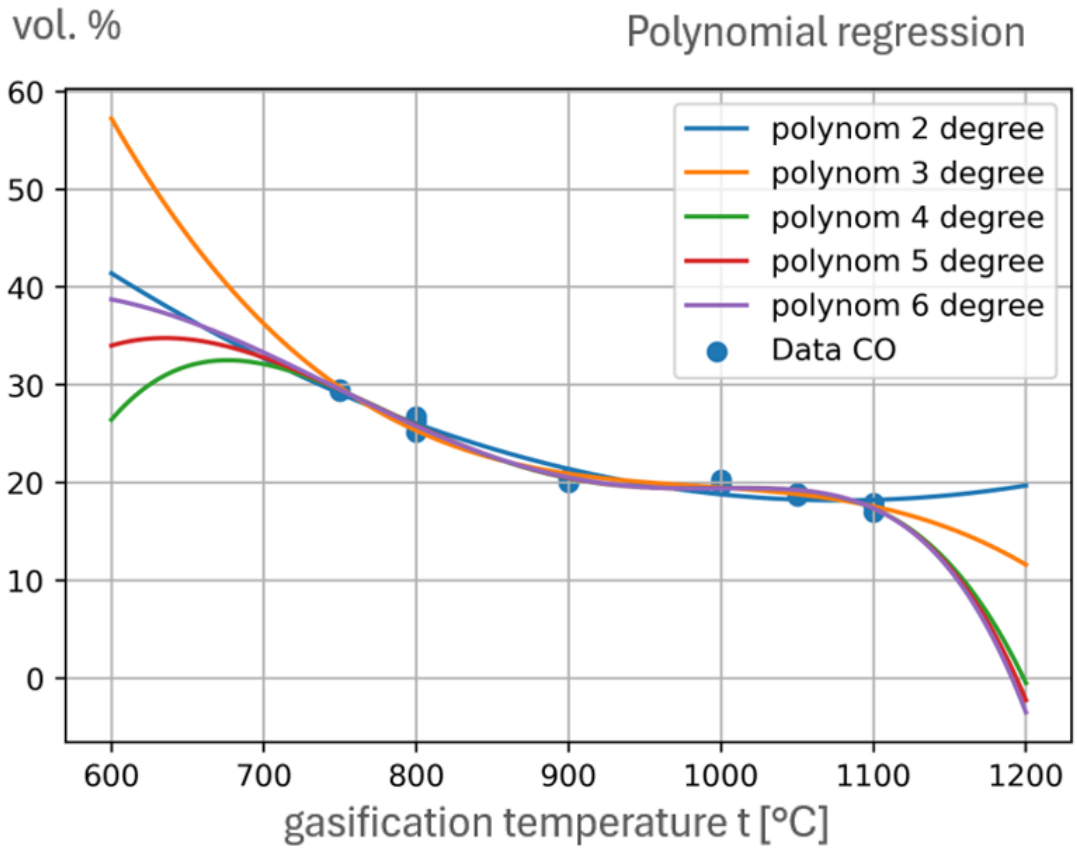

Figure 11. Volumetric percentage of CO in the gasification reactor: Polynomial regression models valid for 750–1100 °C; volumetric percentage vs. gasification temperature t [°C].

- **Methane CH_4**

The recommended model for methane CH_4 is a polynomial of degree 4, as given in Table 9. Its mean squared error is as low as 0.04.

Table 9. Optimized polynomial formulations between middle reactor temperature (t [°C]) and the amount of produced methane CH_4.

 doi:10.20944/preprints202512.1609.v1

Polynomial degree	Methane CH_4
2	$1.885\times10^{-5}\,t^2-0.045t+27.658$
3	$2.838\times10^{-8}\,t^3-6.012\times10^{-5}\,t^2+0.028t+5.659$
4	$-1.286\times10^{-9}\,t^4+4.803\times10^{-6}\,t^3-0.007t^2+4.06t-911.393$
5	$-1.081\times10^{-12}\,t^5+3.783\times10^{-9}\,t^4-4.659\times10^{-6}\,t^3+0.002t^2+5.032\times10^{-6}\,t-164.977$
6	$-9.135\times10^{-16}\,t^6+3.062\times10^{-12}\,t^5-3.525\times10^{-9}\,t^4+1.421\times10^{-6}\,t^3+4.16\times10^{-9}\,t^2-8.928\times10^{-12}\,t-44.059$

Figure 12 shows optimized models of volumetric percentage of CH_4 in dependence on temperature t [°C] in the gasification reactor obtained in polynomial regression.

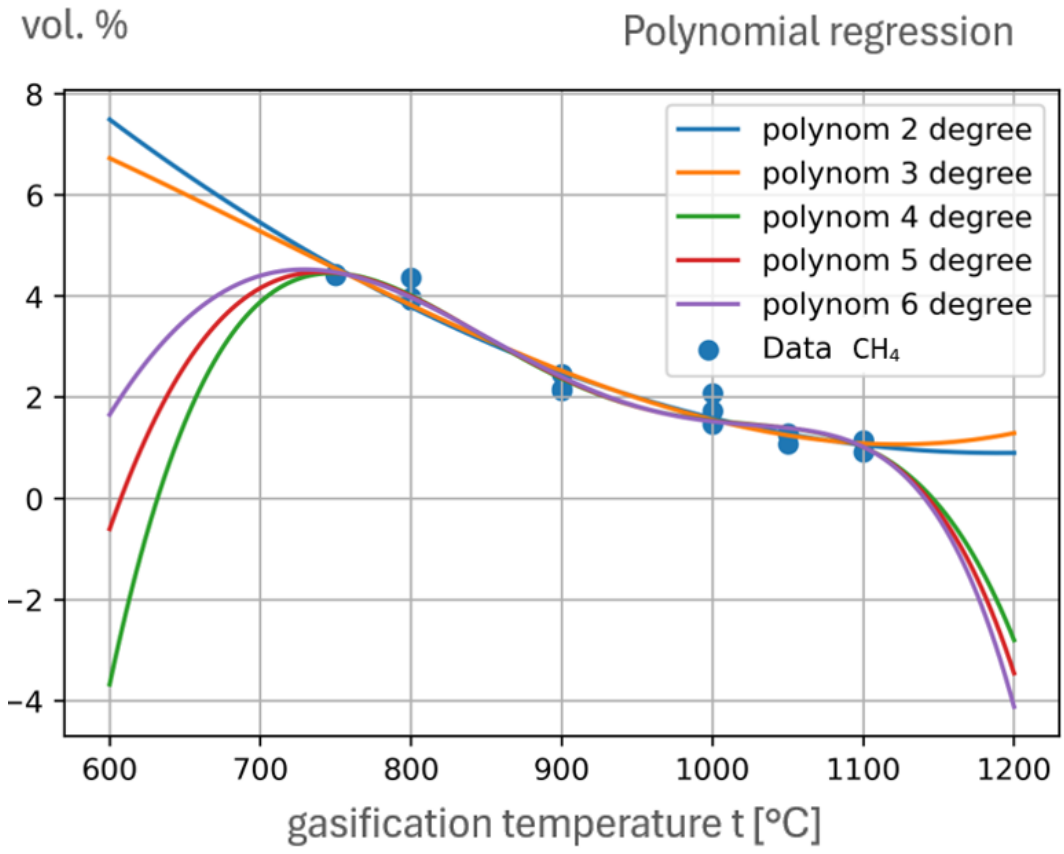

Figure 12. Volumetric percentage of CH_4 in the gasification reactor: Polynomial regression models valid for 750–1100 °C; volumetric percentage vs. gasification temperature t [°C].

- **Nitrogen N_2**

The recommended model for nitrogen N_2 is a polynomial of degree 4, as given in Table 10. Its mean squared error is only 0.49.

Table 10. Optimized polynomial formulations between middle reactor temperature (t [°C]) and the amount of produced nitrogen N_2.

 doi:10.20944/preprints202512.1609.v1

Polynomial degree	Nitrogen N_2
2	$3.801\times10^{-5}t^2-0.037t+51.345$
3	$-2.679\times10^{-7}\,t^3+0.001t^2-0.722t+258.964$
4	$-2.412\times10^{-9}\,t^4+8.687\times10^{-6}\,t^3-0.012t^2+6.841t-1461.047$
5	$-1.941\times10^{-12}\,t^5+6.545\times10^{-9}\,t^4-7.77\times10^{-6}\,t^3+0.003t^2+8.155\times10^{-6}\,t-222.896$
6	$-1.597\times10^{-15}\,t^6+5.167\times10^{-12}\,t^5-5.755\times10^{-9}\,t^4+2.271\times10^{-6}\,t^3+6.647\times10^{-9}\,t^2-1.427\times10^{-11}\,t-34.106$

Figure 13 shows optimized models of volumetric percentage of N_2 in dependence on temperature t [°C] in the gasification reactor obtained in polynomial regression.

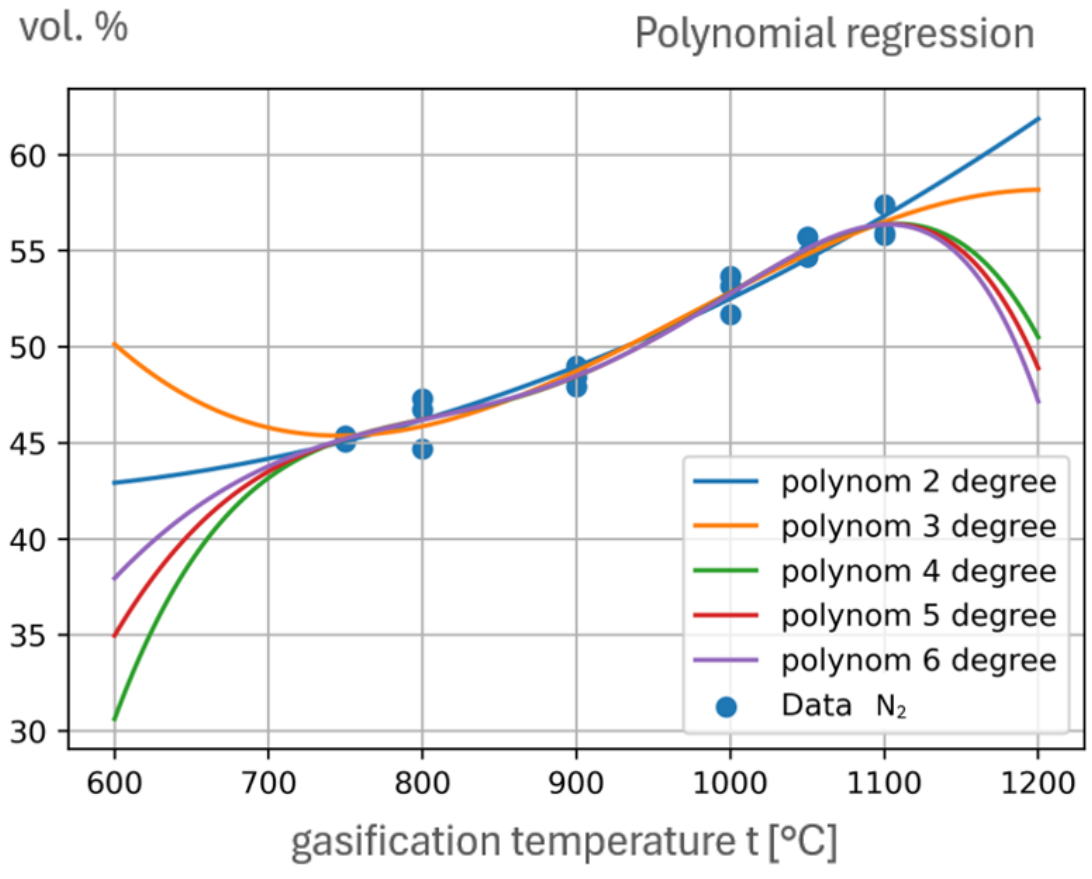

Figure 13. Volumetric percentage of N_2 in the gasification reactor: Polynomial regression models valid for 750–1100 °C; volumetric percentage vs. gasification temperature t [°C].

In summary, recommendations for the optimized models obtained in polynomial regression are presented after analyzing regression polynomials of degrees 2, 3, 4, 5, and 6 with respect to maximum absolute error, maximum relative (percentage) error, and mean squared error, as given in Table 11.

 doi:10.20944/preprints202512.1609.v1

Table 11. Analysis of maximum absolute error, maximum percentage error, and mean squared error for polynomial models of degrees 2, 3, 4, 5, and 6 applied to hydrogen (H_2, Table 6), carbon dioxide (CO_2, Table 7), carbon monoxide (CO, Table 8), methane (CH_4, Table 9), and nitrogen (N_2, Table 10).

Polynomial	degree 2	degree 3	[a] degree 4	degree 5	degree 6
Max. absolute error					
CO_2	1.05	0.69	0.48	0.49	0.51
H_2	1.9	2.09	1.07	1.13	1.18
CO	1.48	1.43	0.87	0.91	0.96
CH_4	0.57	0.54	0.54	0.55	0.56
N_2	1.51	1.42	1.53	1.52	1.51
Max. relative (percentage) error					
CO_2	13.0	9.0	6.0	6.0	6.0
H_2	20.0	22.0	11.0	12.0	12.0
CO	9.0	8.0	5.0	5.0	6.0
CH_4	62.0	57.9	59.0	60.0	61.0
N_2	3.0	3.0	3.0	3.0	3.0
Mean squared error					
CO_2	0.27	0.07	0.04	0.04	0.04
H_2	1.09	0.87	0.3	0.35	0.39
CO	0.75	0.35	0.21	0.22	0.23
CH_4	0.06	0.06	0.04	0.04	0.05
N_2	0.63	0.54	0.49	0.49	0.49

[a] recommended for use

2.1.4. Hydrogen Separation

Separation of hydrogen is very important because fuel cells require very clean fuel.

The maximum production of hydrogen is achieved for different combinations of inputs for the plasma torch as given in Table 12. Different combinations of the input parameters can give the same output values.

Table 12. Input combinations for the plasma torch optimized for maximum hydrogen production H_2.

	Inputs[a]			Outputs [b]			
Combination	k [-]	P [kW]	f_P [bar]	T [K]	t [°C]	[c] Syngas	vol.

 doi:10.20944/preprints202512.1609.v1

						produced [m³/h]	H_2 %
1.	9.6	15	3	10621.9	925	17.6	15.9
2	5	9.9	3.8	10621.9	925	17.6	15.9
3	8.9	15	3.3	10429.3	921.3	17.6	15.9
4	5	7.5	3	10225.0	917.4	17.6	15.9
⋮	⋮	⋮	⋮	⋮	⋮	⋮	⋮

[a] the base constant of nozzle k [no units] from 5 to 20, required power of plasma torch P [kW] from 5 to 15, and filling pressure [bar] from 3 to 8 Used unrealistic peak in symbolic regression is 22.5 % vol. of hydrogen; [b] T [K] is the middle temperature of the plasma torch, while t [°C] is the temperature in the gasification reactor; [c] for waste input 20 kg/h (e.g., waste input 5 kg/h gives 4.4 m³/h of syngas)

The actual physical method used for separating hydrogen and its purification is not relevant for this evaluation.

2.1.5. Hydrogen Tank

After separation and compression, the hydrogen is stored in bundles of high-pressure cylinders forming a hydrogen tank. The hydrogen tank attached to the gasification facility has the volume of 2.2 m³, with pressure of 20 MPa (200 bar), and with the temperature in the tank of 298 K. In this tank with these parameters, n≈17758 mol can be placed inside, which means ~ 35.52 kg of hydrogen. If the production of hydrogen is 0.39 kg/hour, then around 92 hours or around 3.84 days are needed to fill the tank [52]. This tank is shown in Figure 14; the white bottles are filled with hydrogen produced in the facility, while the red bottles are filled with pure hydrogen with certified cleanliness bought on the market for comparison with the produced one.

Figure 14. Hydrogen storage tanks installed in the gasification facility

An example of the filling duration of a hydrogen tank is given in Table 13.

Table 13. Estimated filling duration of hydrogen tank connected to the gasification system.

k	P	f_p	Waste	Syngas	vol.	H_2	Tank		
[-]	[kW]	[bar]	input [kg/h]	produced [m³/h]	H_2 %	produced [m³/h]	Pressure [bar]	Temperature [K]	Filling time

 doi:10.20944/preprints202512.1609.v1

									[h]
9.6	15	3	20	17.6	15.9	2.79	100	200	107
5	9.9	3.8	5	4.4	15.9	0.70	160	220	623
8.9	15	3.3	10	8.8	15.9	1.40	200	250	343
8.9	15	3.3	17	15.0	15.9	2.38	200	298	169
13.4	9.4	6.4	16	14.1	10.5	1.48	200	298	276
9.7	11.3	4.9	20	17.6	12.8	2.25	200	298	182
⋮	⋮	⋮	⋮	⋮	⋮	⋮	⋮	⋮	⋮

 doi:10.20944/preprints202512.1609.v1

2.1.6. Fuel Cells and Electrolyzers

2.1.6.1. Fuel Cells

Fuel cells are electrochemical devices that convert the chemical energy of a fuel, typically hydrogen, directly into electricity through a reaction with oxygen (from ambient air), producing water and heat as byproducts. They are highly efficient and environmentally friendly, with applications ranging from powering vehicles to providing electricity for buildings and portable devices.

It is estimated that around 0.3 kg of hydrogen which can be produced per hour from the gasification facility can give around 10.2 kWh of electrical energy (lower heating value - LHV) or 12.2 kWh of electrical energy (higher heating value - HHV). These values are for 100% fuel cell efficiency. When used as part of a fuel cell, 1 kg of hydrogen can produce 33 kWh/kg of electrical energy (lower heating value - LHV) for high-temperature fuel cells if the product is steam, or 39.38 kWh/kg (higher heating value - HHV) for low-temperature fuel cells if the product is water in liquid phase. In a low-temperature fuel cell, where the product is liquid water, the HHV should be employed in efficiency calculations, while for high-temperature fuel cells, it may be permissible to use the LHV if the product steam is put to good use [53]. Efficiency (35 %-60 %): 3.57 kWh of electrical energy (lower heating value - LHV), 4.26 kWh of electrical energy (higher heating value - HHV) - Both in real conditions [54][2].

The installed fuel cells are in 5 stacks of 8 kW and are connected directly to the electric grid.

The examples of work of fuel cells installed within the observed gasification facility are given in Table 14.

Table 14. Operating Inputs and Outputs of the Fuel Cell Unit.

k [-]	P [kW]	f_p [bar]	Waste input [kg/h]	Mass of H_2 [kg/h]	[a] Power of fuel cells [kW]	Efficiency [%]	Output — Obtained electrical energy [kWh]	
							[b] LHV=33kWh/kg	[c] HHV=39.38kWh/kg
9.6	15	3	20	0.39	40	50	6.4	7.6
5	9.9	3.8	5	0.10	40	40	1.3	1.5
8.9	15	3.3	10	0.17	40	36	2.0	2.4
8.9	15	3.3	17	0.29	40	36	3.4	4.1
13.4	9.4	6.4	16	0.13	40	60	2.6	3.1
9.7	11.3	4.9	20	0.19	32	60	3.7	4.4
⋮	⋮	⋮	⋮	⋮	⋮	⋮	⋮	⋮

[a] In up to 5 stacks of 8 kW; [b] LHV is Lower Heating Value; [c] HHV is Higher Heating Value

The installed fuel cells are shown in Figure 15.

[2] Table 3 of [54] gives also specific types of low- and high-temperature fuel cells and their efficiency

 doi:10.20944/preprints202512.1609.v1

Figure 15. Installed Nedstack FCS 8-XXL fuel cell stacks as part of the system for hydrogen-to-electricity conversion

2.1.6.2. Electrolyzer

An electrolyzer is a device that uses electricity to split water into hydrogen and oxygen through a process called electrolysis [55,56]. The technology in fuel cells and electrolyzers is related but operates in reverse mod. While fuel cells generate electricity by combining hydrogen and oxygen, producing water as a byproduct, electrolyzers use electricity to split water into hydrogen and oxygen.

Typically, 52 kWh are required to produce 1 kg of hydrogen[3]. Therefore, 3.57 kWh produced typically per hour in fuel cells can produce 0.069 kg of hydrogen. This means that around 22.21% of hydrogen can be recovered if the hydrogen is used to produce electricity in fuel cells and then to use this produced electricity to produce hydrogen in the electrolyzer.

The implemented models are general and, therefore, offer calibration according to the requirements of researchers.

The electrolyzer has the power of 14 kW. It is shown in Figure 16. The installed electrolyzer is not connected to the electric grid, but the electric energy is instead supplied through photovoltaics of 170kW and wind turbines of 10kW.

[3] Electrolyzer modeling for green hydrogen: https://www.gridcog.com/blog/electrolyser-modelling-for-green-hydrogen (accessed on June 28, 2024)

 doi:10.20944/preprints202512.1609.v1

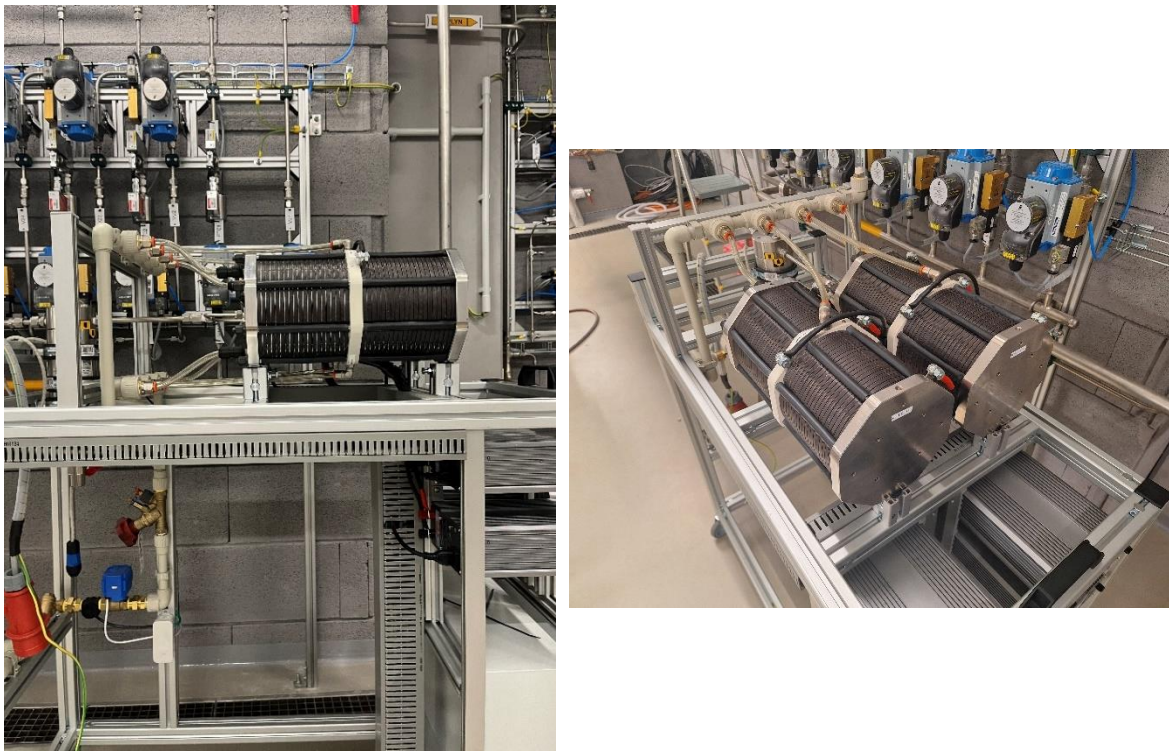

Figure 16. Acta AES 1000 electrolyzer integrated into the facility to produce hydrogen from water electrolysis

The installed electrolyzer is used as an auxiliary process for producing hydrogen in addition to the gasification of waste, which is the main process for producing hydrogen. The examples of work of the electolyzer are given in Table 15.

Table 15. Operating inputs and outputs of the electrolyzer unit.

[a] Electricity input [kWh]		Hydrogen produced [kg]	
Photovoltaics and wind	Grid	From photovoltaics and wind	From grid
14	54	0.27	1.04
20	20	0.38	0.38
17	7	0.33	0.13
⋮	⋮	⋮	⋮

[a] Energy required to produce 1 kg of H_2 =52 kWh, H_2 produced from 1 kWh of electricity =0.02kg

2.1.6.3. Purge Process of Fuel Cells and Electrolyzers

The purge process for fuel cells has also been developed (it is valid for electrolyzers as well). Validation of fuel cells and electrolyzers was performed in R programming language, and a script for fuel cell validation (detection and prediction of purge) and a script for electrolyzer validation (detection and prediction of pressurization and hydrogen generation) were implemented in-house[4].

The purge is a cleaning process whereby the short-term opening of the hydrogen valve at the output of the fuel cell modules washes away impurities from the anode side of the cells, thus stopping the gradual drop in their operating voltage.

[4] These scripts are given in Appendix B

 doi:10.20944/preprints202512.1609.v1

Pressurization occurs in the production of hydrogen, when a constant increase in pressure is sharply reduced at some point. In addition to finding where this reduction occurred, the total amount of hydrogen produced between two moments of pressurization is also of interest. In both cases, it is a problem of detecting changes in time series. In order to automate and facilitate the work, it was also necessary to create a set of custom scripts in the R language to ensure that the results could be easily retrieved and converted into a user-friendly form and saved to a disk.

The selected methods for both fuel cell purge time detection and electrolyzer pressurization detection are of two types, with the first one being based on the use of sliding windows and the calculation of the average values in these windows. The difference of these values in two adjacent windows is then used to identify the change. The second method relies on the widely used Bayesian approach and the use of Markov Chain Monte Carlo (MCMC) simulation. This modern method produces a probabilistic time series profile based on the input data and using MCMC simulation. From this profile, the change points are extracted using the created scripts, which are then displayed to the user.

Figure 17 shows the results of the algorithm for detecting fuel cell purges. The results show that the fuel cell purge detection is highly reliable for the detection task, as it produces only three false positives.

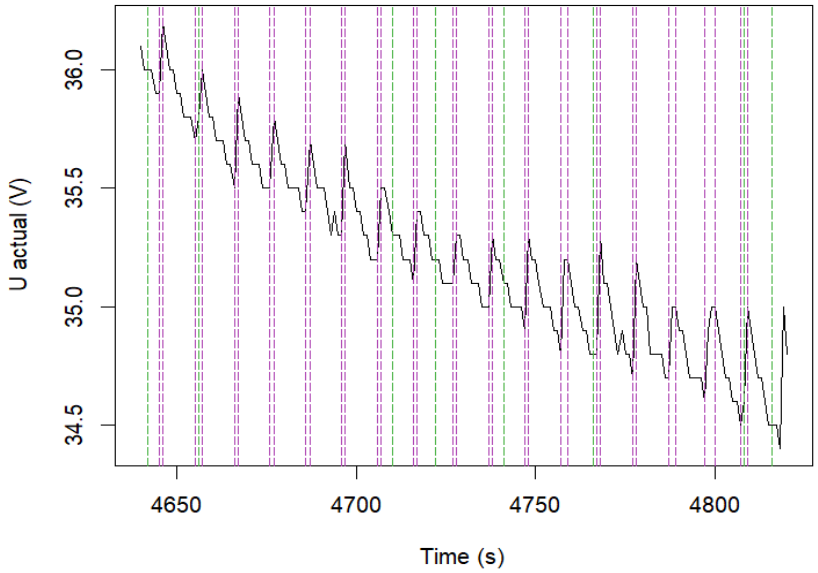

Figure 17. Results of the fuel cell purge detection algorithm. purple indicates the known start and end of purges, while green shows the algorithm-predicted values

Table 16 shows the comparison of the known values with the values predicted by the algorithm electolyzers.

Table 16. Electrolyzer pressurization detection: algorithm performance results.

[a]Amount of hydrogen produced

Interval	Actual (dm^3/min)	Prediction (dm^3/min)	Absolute error (dm^3/min)
1	40.73	40.73	0
2	20.69	20.63	0.06

 doi:10.20944/preprints202512.1609.v1

3	19.75	19.83	0.08
4	29.84	29.84	0
5	28.02	28.01	0.01
6	28.78	28.56	0.22
7	28.40	28.68	0.28
8	30.39	32.92	2.53
9	2.62	0.09	2.53
10	26.28	28.53	2.25
11	36.70	34.06	2.64
12	29.69	30.23	0.54
13	31.39	31.18	0.21
14	30.75	31.08	0.33
15	34.79	34.79	0
16	30.23	30.23	0

[a] Expressed in dm^3, i.e. in liters, under normal conditions of pressure and temperature

The calculated absolute error shows that the algorithm can predict the values of hydrogen produced quite accurately: out of 16 intervals, in 12 cases the algorithm predicted the amount of hydrogen produced with an absolute error of less than 0.54 dm^3/min (cases are shown in green). The maximum error of the algorithm was in 11 intervals: the algorithm predicted the amount of hydrogen produced to be 28.53 dm^3/min, while the reality was 26.28 dm^3/min. This corresponds to an absolute error of 2.64 dm^3/min.

2.1.7. Combustion or Production of Liquid Fuel — An Alternative Process in the Gasification Facility

The synthesis gas produced can be used in two ways. The first is its energy recovery. That is, it is burned in a suitable energy device (burner, turbine, boiler, etc.) and thus, the chemical energy is converted into chemical energy.

Table 17 shows the amount of gases and related energy if all combustible components of syngas produced from 60kg of waste per hour (if the entire produced amount of all combustible compounds of gas, including hydrogen, go into combustion).

Table 17. Amounts of Gases and Associated Energy from Syngas Generated from 60 kg/h of Waste.

[a] Component of syngas	Produced kg/hours	Ideal theoretical 100% efficiency		35% efficiency	
		kWh – HHV	kWh – LHV	kWh – HHV	kWh – LHV

 doi:10.20944/preprints202512.1609.v1

H_2	0.53	21.05	17.79	7.37	6.23
CO	16.88	47.63	47.63	16.67	16.67
CH_4	1.39	21.34	19.21	7.47	6.72

[a] HHV Higher Heating Value: H_2=142.08 MJ/kg, CO=10.16 MJ/kg, and CH_4=55.38 MJ/kg; LHV Lower Heating Value: H_2=120.08 MJ/kg, CO=10.16 MJ/kg, and CH_4=49.85 MJ/kg – The higher and lower heating values are the same if their hydrogen compound content is zero because no water is produced neither in vapor nor in liquid phase [57].

The second option is to use syngas to produce liquid fuel. The liquid fuel is most often prepared by the synthesis of CO and H_2 on a suitable catalyst [58-60]. Since syngas contain components other than CO and H_2, these components must be suitably separated from the gas and subsequently transformed to CO and H_2 using reforming (steam or dry). The N_2 component, which comes from the gasification medium, must be separated as it has no energy value.

2.1.8. Photovoltaics and Wind Turbine

Photovoltaics of up to 170 kW and wind power of up to 10 kW are installed to provide power for the electrolyzer. Surpluses of electric energy are stored in the PYLONTECH LiFePO4 battery with the capacity of 500 kWh.

The installed photovoltaics and wind turbines are shown in Figure 18. Time to fill up the battery from such photovoltaics and wind turbines is given in Table 18.

Figure 18. Photovoltaic and wind energy systems installed in the facility

Table 18. Electricity input and output of the system with the corresponding times required to fully charge the battery.

Electricity from		Battery capacity [kWh]	[a] Consumed by	
Photovoltaics [kW]	Wind turbine [kW]		Battery [kWh]	Time to fill up the battery [hours]
120	5	500	108	4.6
60	7	500	50	10

 doi:10.20944/preprints202512.1609.v1

60	7	600	50	12
120	3	700	106	6.6
⋮	⋮	⋮	⋮	⋮

[a] The electolyzer consumes 17kWh.

2.2. Small Pyrolysis

An additional separate facility, i.e., the secondary facility in the examined waste-to-energy system includes small pyrolysis, the diagram of which is given in Figure 19. The main product of pyrolysis is liquid fuel - pyrolysis oil [61-63], while the byproduct is gas and char, the composition of which is very different compared with the gas produced in the gasification facility, i.e., in the primary facility.

Pyrolysis oil is a very heterogeneous substance consisting of many compounds [64], which can be dangerous for the environment and humans [65, 66]. However, with appropriate handling, this danger can be eliminated so that pyrolysis liquid can be a valuable source of raw materials [67].

Small pyrolysis is designed for 2-5 kg of waste per hour with the maximum outputs for 5 kg of waste: Char up to 1.9 kg/hour, liquid fuel, i.e., pyrolysis oil 1.6 kg/hour, and gases 1.5 kg/hour (very different composition of gas compared with gasification). The volume of this produced gas under normal conditions of pressure and temperature is around 0.9 m^3.

The diagram of the installed small pyrolysis is shown in Figure 19 and a photo of the installed small pyrolysis is in Figure 20.

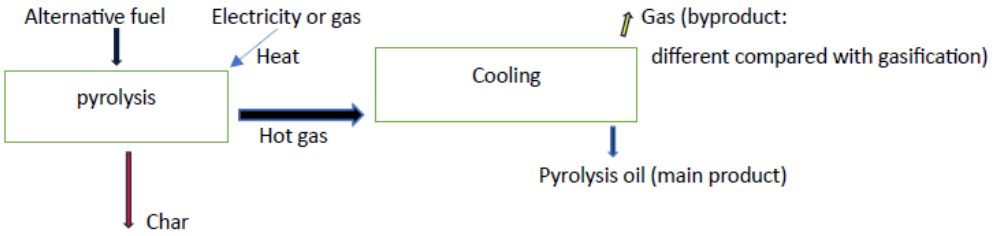

Figure 19. Diagram of the small pyrolysis unit, the secondary facility of the waste-to-energy system.

Figure 20. Installed small-scale pyrolysis unit.

 doi:10.20944/preprints202512.1609.v1

The input/output relations within the processes of the pyrolysis facility are identified in Table 19.

Table 19. Operational input–output relations of the pyrolysis as the secondary facility of waste-to-energy system

	Input	Output
Pyrolysis reactor	Alternative fuel – Waste	Hot gas
	Heat (through electricity or gas)	Char
Cooling	Hot gas	Pyrolysis oil (liquid fuel) — Main product
		Syngas (different than syngas from gasification) — Byproduct

The temperature of pyrolysis is given in Equation (3):

$$t=(p+1.5591)/0.0425 \quad (3)$$

Where t is temperature [°C] (from 300 °C to 800 °C), and p is energy consumed in pyrolysis [MJ] (from 3.6MJ to 36MJ).

Five kg of waste gives 3.06m^3 of gas in pyrolysis if all mass is transformed into gas (it is based on the logic from gasification for mass balance) – 100% of mass in gas is not possible in practice because gas is a by-product. Based on [31], this amount of gas is corrected giving 0.91m^3 of gas: CO=0.287m^3, CO_2=0.548m^3, CH_4=0.075m^3, and H_2=0.0006102m^3. 1.489 kg of the total mass of input waste is transformed into gas.

Mass percentage of gas G is given in Equation (4):

$$G_{\%mass} = 11.3943 + 0.059\times t \quad (4)$$

Where t is pyrolysis temperature [°C].

Mass percentage of gas compounds is given in Table 20.

Table 20. Mass percentage of individual gas compounds produced by pyrolysis [a].

Gas compound	mass. %
CO_2	$76.631-0.0309\times t-0.000070876\times t^2$
CO	$71.64571-0.18489\times t+0.00018\times t^2$
CH_4	$-35.957+0.1855\times t-0.00014\times t^2$
H_2	$-10.5349+0.0235\times t+0.0000336\times t^2$

[a] t is pyrolysis temperature [°C]

mass percentage of liquid fuel (pyrolysis oil) L is given in Equation (5):

$$L_{\%mass} = 30.2507+0.0246\times t-0.000057833\times t^2 \quad (5)$$

 doi:10.20944/preprints202512.1609.v1

Where t is pyrolysis temperature [°C], while the rest, aside from the liquid and gas part, is biochar.

The examples from small pyrolysis are given in Table 21.

Table 21. Sample results from laboratory-scale pyrolysis.

Input			Output			
Electricity [kWh]	Waste [kg/h]	Pyrolysis temperature t [°C]	Pyrolysis oil (Liquid fuel) L [kg]	Char [kg]	Gas G [kg]	
5.4	3	494.1	0.85	1.16	0.99	Example 1
3.3	5	316.2	1.61	1.50	1.89	Example 2
⋮	⋮	⋮	⋮	⋮	⋮	⋮

Table 22 examines, in more detail, Examples 1 and 2 from Table 21 for by-product Gas G.

Table 22. Examples 1 and 2 demonstrating by-product gas composition from Table 21

Example 1	Composition Vol. %	Volume [m³]	Mol	Mass [%]	Mass [kg]
CO_2	44.5	0.3	14.6	65.1	0.64
CO	24.5	0.2	8.0	22.8	0.23
CH_4	21.7	0.2	7.1	11.6	0.11
H_2	9.4	0.1	3.0	0.6	0.01
Σ	**100**	**0.7**	**32.9**	**100**	**0.99**
Example 2	Composition Vol. %	Volume [m³]	Mol	Mass [%]	Mass [kg]
CO_2	59.8	0.5	24.5	72.2	1.08
CO	31.2	0.3	12.7	24.0	0.36
CH_4	8.7	0.1	3.5	3.8	0.06
H_2	0.3	0.0	0.1	0.0	0.00
Σ	**100**	**0.9**	**41.0**	**100**	**1.5**

 doi:10.20944/preprints202512.1609.v1

3. Conclusions

This study developed and deployed open-source regression-based software tool for simulating compact, mobile, and user-friendly waste-to-energy facilities. The objective was to support planning, development, management, and optimization of waste management in the Czech Republic and beyond.

Key quantitative findings

- Gasification: Regression methods provided interpretable and robust approximations of thermochemical processes of transforming waste to syngas, contrasting with black-box deep learning approaches. Furthermore, polynomial regression models perform better in this case compared to symbolic regression models. Optimal reactor temperature range was determined as 879–966 °C, with a peak hydrogen yield at 923 °C (H_2 = 15.1%, CO_2 = 11.87%, CO = 19.76%, CH_4 = 2.11%, N_2 = 49.3%, total 98.78%).
- Pyrolysis: the developed model identified an optimal power of 3.3 kW, converting 3 kg/h of waste input into 0.97 kg/h of liquid fuel.

Limitations

- Current validation is limited by the availability of experimental datasets.
- The results are based on wood pallets typical of Central Europe; feedstock variability may affect accuracy when extending to other waste types.
- Scaling up from laboratory to industrial operation may introduce additional uncertainties related to reactor performance, energy efficiency, and emissions.
- Potential environmental and health impacts of different waste-to-energy processes require further investigation.

Practical and technical implications

- The developed tools are open-source (Python, MS Excel) and accessible through web browsers, enabling interactive scenario analysis.
- The software supports community-scale applications, including industrial enterprises and municipalities, and may be integrated with renewable energy sources (PV, wind) or fuel cell systems.

Future work

- Extend datasets and validation across different waste feedstocks to improve generalizability.
- Conduct a comprehensive techno-economic analysis (similar as Rizqi [5]) to assess feasibility at different scales. Integrate cost analysis.
- Integrate environmental impact assessments (e.g., life-cycle analysis, emission control studies) into the modeling framework.
- Facilitate further transparency by releasing additional open-source data and codes.

 doi:10.20944/preprints202512.1609.v1

Appendix A - Evaluation of gasification models using entropy

An extended analysis for new models based on [47] is given here.

This Appendix A summarizes validation of the developed gasification models by approximation and sample entropy methods.

Various approaches, such as classical polynomial regression and alternative symbolic regression using artificial intelligence elements, were developed and tested. Despite subsequent validation of the models on new data, it appears that statistical criteria such as mean square error (MSE) or Pearson correlation coefficient are not sufficient to select the appropriate model. Therefore, a new model selection methodology was developed based on the measurement of system complexity using entropy.

A new tool was developed using open-source libraries to identify appropriate ("quality") models. The research aimed at developing software that automatically identifies and discards "unsuitable" models. The developed software was tested on gasification models, but due to its generality, it can be tested and used on other models as well.

The developed software identifies "suspicious" models that are of "low quality" according to dynamical systems theory (among others, by using approximation and sample entropy).

A.1 Approximation and sample entropy

The main tools in the software under development to detect model fit are approximation (E_{app} or $ApEn$) and sample entropy (E_{samp} or $SampEn$). In this work, the open-source EntropyHub package [69] for the Python programming language was used for the computation. These methods have already been investigated and applied by many authors for measuring and comparing complexity [70-73].

The entropy values reflect the presence of repeating patterns in the time series. A time series containing many repeating patterns has a small entropy value; data from a less predictable process has a higher entropy value.

A.2 Calculation of approximate entropy

Two parameters are chosen to calculate the approximate entropy:

- m - window length or dimension,
- r - area diameter or tolerance.

Given an input data vector $X = x_1, x_2, \dots, x_N$, an m-dimensional space is constructed using the elements:

$u_m(i) = [x(i), x(i+1), \dots, x(i+m-1)]$.

The number $C_i^m(r)$ is then determined, which is the number $u_m(j)$ such that $d(u_m(i), u_m(j)) \le r$, divided by $N - m + 1$.

The maximum metric is used, thus $d(p,q) = \max_a |p(a) - q(a)|$.

The next step is to determine $\Phi^m(r) = (N-m+1)\sum_{i=1}^{M-m+1} \ln(C_i^m(r))$.

The approximate entropy is finally calculated as $E_{app}(X,m,r) = \Phi^m(r) - \Phi^{m+1}(r)$.

A.3 Calculation of sample entropy

 doi:10.20944/preprints202512.1609.v1

Sample entropy uses the same parameters m and r as the approximation entropy. The algorithm begins in the same way - for the input vector is computed with the m-dimensional elements $u_m(i) = [x(i), x(i+1), \ldots, x(i+m-1)]$.

Sample entropy is defined as $E_{samp}(X, m, r) = \ln \frac{A}{B}$, where:

- A is the number of pairs of vectors such that $d^c\left(u_{m+1}(i), u_{m+1}(j)\right) < r$,
- B is the number of pairs of vectors such that $d^c\left(u_m(i), u_m(j)\right) < r$,
- d^c is the Chebyshev distance.

A.4 Choice of approximation and sample entropy parameters

The approximation and sample entropy parameters are the dimensions m and tolerances r. In order to choose the appropriate parameters for the CEET models, simulations were performed for different values of these parameters. Their dependence on the length of the input data vector, in particular, was also investigated. Considering the nature of the data, the parameter values were chosen as $m = 1$ and $r = 0.2 \times SD$, where SD denotes the standard deviation of the input data. Changes in the parameter r as a function of the length of the input data n are shown in Figure A.1.

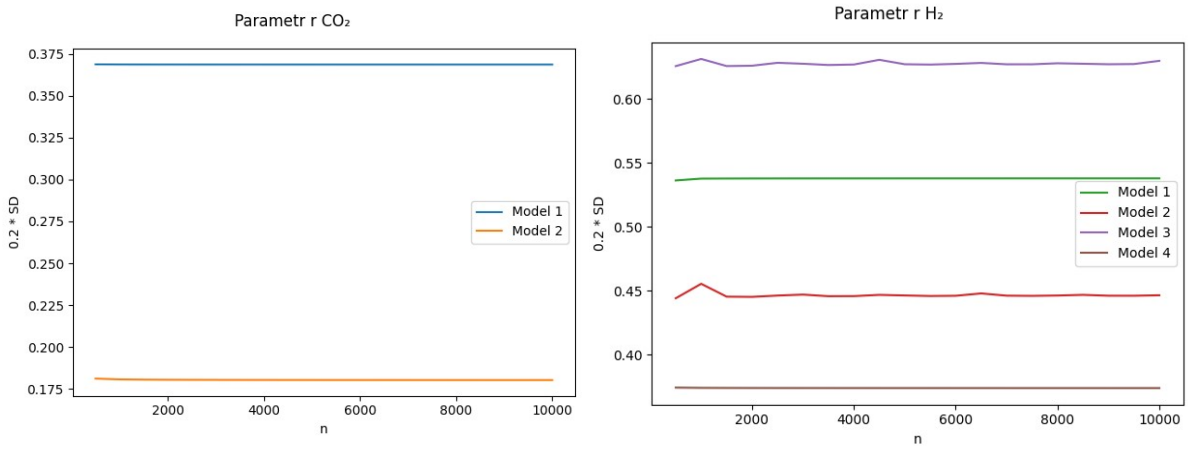

Figure A.1: The plot of the parameter r as a function of the input data length n for CO_2 models (left) and H_2 models (right). Increasing n does not result in significant changes in the parameter values.

On the tested models, it can be seen that the parameter r is not significantly influenced by the length of the tested vector (number of split points of the tested interval). Option $r = 0.2 \times SD$, therefore, does not affect the entropy results.

Subsequently, the focus is on the values of the parameter m (dimension) and entropy values as a function of the input data vector length n. Plots showing the dependence of the approximation entropy values $ApEn$ and sample entropy $SampEn$ as a function of n are presented in Figures A.2 and A.3. Both entropies are calculated for the parameter choices $m = 1$ a $m = 2$. From the plots, it can be concluded that the choice of the parameter m does not affect the nature of the output of the decision mechanism. There is a slowdown in convergence, but it is negligible for the increasing length of the test vector. The choice of the parameter m will therefore not affect the entropy results.

It is also observed that the outputs of both algorithms ($ApEn$ and $SampEn$) are consistent, i.e., the entropy results converge to similar values starting from a certain value of n. It is noted that these are two different algorithms to calculate the same model characteristic - the complexity measure. Therefore, it is important that both algorithms (even given different parameters) give similar results.

 doi:10.20944/preprints202512.1609.v1

The plot of changes in entropy values against the varying length of the input vector n is shown in Figure A.2 (for CO_2) and Figure A.3 (for H_2).

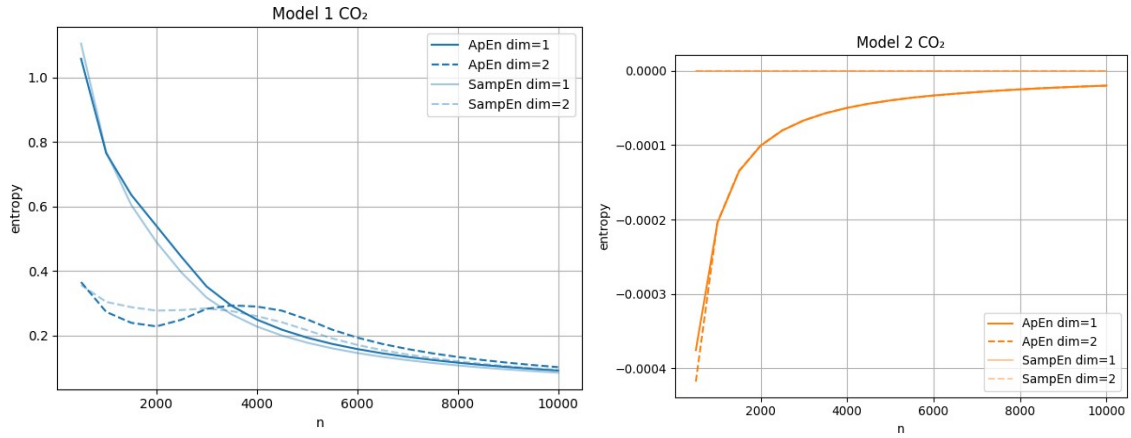

Figure A.2: The plot of dependence of $ApEn$ and $SampEn$ values on the length of the input vector n for two choices of the parameter m (dimension) for CO_2 models.

A.5 Conclusions of model evaluation using entropy

Within the framework of our research, the methods of approximate entropy ($ApEn$) and sample entropy ($SampEn$) were used for a detailed evaluation of the following gasification models :

- CO2 Model 1: $\text{logm}_{10}(t\, e^{\sin(t+0.6718609)})^2$,
- CO2 Model 2: $\text{logm}(-0.060511474\, t^2) + 2.0503674$,
- H2 Model 1: $\frac{8.9065269419}{\cos(\cos(e^{\sin(t+1)}-2))}$,
- H2 Model 2: $\text{logm}_2\left(7.744805\, \left(-9.837645 + \text{logm}(t)\right)^{-1.5165994}\right) + 0.0054770974\, t$,
- H2 Model 3: $6.5368786 + \text{logm}_2(\left|-9.864973 + \text{logm}_2(t)\right|^{-2.1570945})$,
- H2 Model 4: $8.64427756 \times 10^2 - 1.11535475 \times 10^{-2}\, t^2 + 2.50417715 \times 10^{-5} t^3 - 2.08318518 \times 10^{-8} t^4 + 6.0929057 \times 10^{-12} t^5$.

Symbolic regression models (i.e., all models analyzed here except "H2 Model 4") are not numerically stable: the curves of the models are sensitive to the sample length n. The algorithms for calculating entropy themselves depend on the choice of input parameters. Therefore, both algorithms are used for different combinations of the sample length n and for different input parameters to the entropy calculation algorithms (dimension m, tolerance r). The results of the entropy analysis clearly show that the standard algorithm settings are $m = 2, r = 0.2\, S$. The sample length n remains an important variable that affects the entropy values. Knowledge of these characteristics can be used in the future to implement automatic model evaluation.

 doi:10.20944/preprints202512.1609.v1

Table A.1 Entropy values for CO_2 models for n = 10 000

CO_2	ApEn	SampEn
Model 1	0.10207402716557201	0.09283472789592226
Model 2	-1.9966127829285085e-05	0.0

Table A.2 Entropy values for H_2 models for n = 10 000

H_2	ApEn	SampEn
Model 1	0.20472909404756345	0.06955908463228219
Model 2	0.003898864346688402	0.0009846446174318114
Model 3	0.0040850415534996465	0.0010645168626448073
Model 4	0.001447427615602681	0.0013493376152297486

Based on the values of the parameters and entropy (see Tables A.1 and A.2), the models can be evaluated as follows.

For CO_2, Model 1 is more "complex" than Model 2, as can be seen from the higher values of standard deviation (SD) and entropy.

As for H_2, Model 1 shows the highest complexity (approximate entropy of about 0.2). The complexity of Models 2 and 3 is approximately identical, as indicated by the entropy curves, which are very similar. In terms of the lowest complexity, Model 4 (created by polynomial regression) is the best performing one. It achieves the lowest value of approximation entropy, while the value of sample entropy is comparable to Models 2 and 3, see Table A.2. The results for Model 4 are least dependent on the choice of the algorithm (approximation or sample entropy), the parameter m, and the model achieves the lowest value of standard deviation. This is also evident from the plot, see Figure A.3 - Model 4 H_2, where we see all four curves having almost identical forms for both approximation and sample entropy (depending on the length of the input data n and the dimension parameter m). Thus, the best model describing hydrogen gasification is Model 4. For this reason, modeling hydrogen gasification using polynomial regression is recommended.

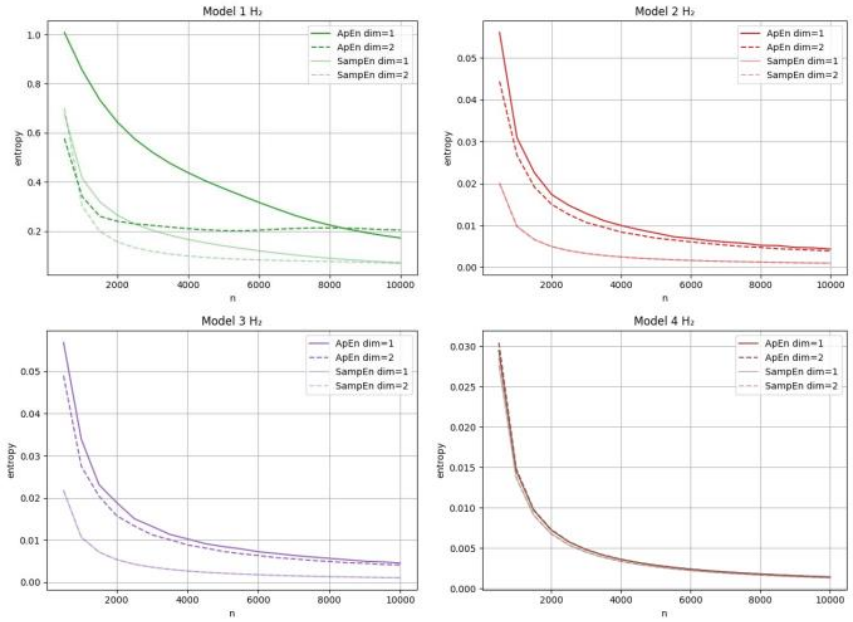

Figure A3. The plot of dependence of $ApEn$ and $SampEn$ values on the length of the input vector n for two choices of the parameter m (dimension) for H_2 models.

 doi:10.20944/preprints202512.1609.v1

A Python script showing these entropy results for hydrogen gasification (H2 Model 4) is described below. The Python script leverages the open-source EntropyHub library. A modification for the other gasification models can be easily provided by a modification of the function "gasification_model(x)".

```
##### Python script for entropy results for hydrogen gasification (H2 Model 4)  #####

### Requirements: python 3.11, EntropyHub 2.0, numpy 2.0.0, matplotlib 3.9.1 ###

import EntropyHub as eh
from numpy import linspace
import matplotlib.pyplot as plt

def gasification_model(x):  ## modify the expression of the gasification model here
    return 8.64427756e+02 + 0.00000000e+00 * x + (
        -1.11535475e-02) * x ** 2 + 2.50417715e-05 * x ** 3 + (
        -2.08318518e-08) * x ** 4 + 6.09290570e-12 * x ** 5

start_t = 750.0
end_t = 1100.0

apen1 = []
apen2 = []
sampen1 = []
sampen2 = []

for count in range(500, 10001, 500):
    t = linspace(start_t, end_t, count)
    v = list(map(gasification_model, t))

    Ap1, Phi1 = eh.ApEn(v, m=1)
    apen1.append(Ap1[1])
    Ap2, Phi2 = eh.ApEn(v, m=2)
    apen2.append(Ap2[2])
    Samp1, A, B = eh.SampEn(v, m=1)
    sampen1.append(Samp1[1])
    Samp2, A, B = eh.SampEn(v, m=2)
    sampen2.append(Samp2[2])

fig, ax = plt.subplots()
ax.plot(range(500, 10001, 500), apen1, 'C5', linestyle='solid', linewidth=1.5)
ax.plot(range(500, 10001, 500), apen2, 'C5', linestyle='dashed', linewidth=1.5)
ax.plot(range(500, 10001, 500), sampen1, 'C5', linestyle='solid', alpha=0.4, linewidth=1.5)
ax.plot(range(500, 10001, 500), sampen2, 'C5', linestyle='dashed', alpha=0.4, linewidth=1.5)
```

 doi:10.20944/preprints202512.1609.v1


```
ax.set_xlabel('n')
ax.set_ylabel('entropy')
ax.grid(True)
ax.legend(['ApEn dim=1', 'ApEn dim=2', 'SampEn dim=1', 'SampEn dim=2'])
plt.title('Model 4 H\u2082')
plt.show()

############################################################
```

Appendix B

A fuel cell script in the R language related to detection and prediction of purge and an electrolyzer, and the R script related to detection and prediction of pressurization and hydrogen generation are given as follows:

-Fuel cells:

```
##### R script for purge detection of fuel cells #####

### Requirements ###

needed.packages = c("readxl", "zoo","bcp")
new.packages = needed.packages[!(needed.packages %in%
installed.packages()[,"Package"])]
if(length(new.packages)) install.packages(new.packages)

require(readxl)
require(zoo)
require(bcp)
source("get_highs.r")
source("get_lows.r")



### Load and visualize data ###

det_purge = read_excel("purge_detection.xlsx")
begend = c(4645, 4646, 4655, 4657, 4666, 4667, 4676, 4677, 4686, 4687, 4696, 4697, 4706,
4707, 4716, 4717, 4727, 4728, 4737, 4738, 4747, 4748, 4757, 4759, 4767, 4768, 4777, 4778,
4787, 4789, 4797, 4800, 4807, 4809)
plot(`U actual (V)` ~ `Time (s)`, data=det_purge, type = "l")
abline(v=begend, lty = "longdash", col = "red")
val_shift = as.numeric(det_profuk[1,1]-1)



### Sliding window method ###
```

 doi:10.20944/preprints202512.1609.v1


```
sd_purge = rollapply(det_purge$`U actual (V)`, width = 10, by = 1, FUN = sd, align =
"left")
plot(sd_purge, type = "l")
abline(v=begend-val_shift, lty = "longdash", col = "red")
getmaxpurge = get_highs(sd_purge)
plot(`U actual (V)` ~ `Time (s)`, data=det_purge, type = "l")
abline(v=getmaxpurge+val_shift, lty = "longdash", col = "green")


### Bayes method ###

bcp_model = bcp(det_purge$`U actual (V)`, burnin = 10000, mcmc = 100000, p0 = 0.01)
plot(bcp_model$posterior.prob, type = "l", xlab = "Time (s)", ylab = "Posterior
probability (-)")
bcp_purge = get_lows(bcp_model$posterior.prob)
plot(`U actual (V)` ~ `Time (s)`, data=det_purge, type = "l")
abline(v=bcp_purge+val_shift, lty = "longdash", col = "green")


### Save data ###

write.table(getmaxpurge+val_shift, file = "Purge_prediction_windows.csv",
row.names=FALSE, col.names = "Purge time prediction (s)", sep=";", append = FALSE,
quote = FALSE, eol = "\n", dec = ".")
write.table(bcp_purge+val_shift, file = "Purge_prediction_bayes.csv",
row.names=FALSE, col.names = "Purge time prediction (s)", sep=";", append = FALSE,
quote = FALSE, eol = "\n", dec = ".")


##### END SCRIPT #####
```

-Electrolyzers:

```
##### R script for pressurization detection of electrolyzers #####


### Requirements ###

needed.packages = c("readxl", "bcp")
new.packages = needed.packages[!(needed.packages %in%
installed.packages()[,"Package"])]
if(length(new.packages)) install.packages(new.packages)
```

 doi:10.20944/preprints202512.1609.v1


```
require(readxl)
require(bcp)
source("get_highs_p.r")
source("sum_per_int.r")


### Load and visualize data ###

det_press = read_excel("pressure_detection.xlsx")
pressure = c(8690, 8976, 9233, 9602, 9917, 10215, 10458, 10623, 10672, 10802, 10976,
11115, 11258, 11400, 11552)
val_shift = as.numeric(det_press[1,1]-1)
plot(det_press$`output hydrogen pressure (bar)` ~ det_press$`time (s)`, type = "l",
ylab = "Output pressure (bar)", xlab = "Time (s)")
abline(v=pressure, lty = "longdash", col = "red")


### Bayes method ###

bcp_model = bcp(det_press$`output hydrogen pressure(bar)`, burnin = 10000, mcmc
= 100000, p0 = 0.01)
plot(bcp_model$posterior.prob, type = "l", xlab = "Time (s)", ylab = "Posterior
probability (-)")
bcp_press = get_highs_p(bcp_model$posterior.prob, 0.155)
plot(det_press$`output hydrogen pressure(bar)` ~ det_press$`time (s)`, type = "l",
xlab = "Time (s)", ylab = "Output pressure (bar)")
abline(v=bcp_press + val_shift, lty = "dotted", col = "green")
sum_per_int(det_press, bcp_press)


### Save data ###

write.table(bcp_press+val_shift, file = "Pressure_detection.csv", row.names=FALSE,
col.names = "Pressure time prediction (s)", sep=";", append = FALSE, quote = FALSE,
eol = "\n", dec = ".")


##### END SCRIPT #####
```

Author Contribution Roles: Dejan Brkić: Conceptualization, Data curation, Formal Analysis, Funding acquisition, Investigation, Methodology, Software, Supervision, Validation, Visualization, Writing – original draft, Writing – review & editing; **Pavel Praks**: Conceptualization, Data curation, Formal Analysis, Funding acquisition, Investigation, Methodology, Project administration, Resources, Software, Supervision, Validation,

 doi:10.20944/preprints202512.1609.v1

Visualization, Writing – original draft, Writing – review & editing; **Judita Buchlovská Nagyová**: Conceptualization, Data curation, Software, Validation, Visualization, Writing – original draft, Writing – review & editing; **Michal Běloch**: Conceptualization, Data curation, Formal Analysis, Methodology, Software, Validation, Writing – original draft, Writing – review & editing; **Martin Marek:** Conceptualization, Data curation, Formal Analysis, Methodology, Software, Validation, Visualization, Writing – original draft, Writing – review & editing; **Jan Najser**: Conceptualization, Data curation, Formal Analysis, Funding acquisition, Investigation, Methodology, Project administration, Resources, Software, Supervision, Validation, Writing – original draft, Writing – review & editing; **Renáta Praksová:** Conceptualization, Data curation, Formal Analysis, Methodology, Software, Validation, Visualization, Writing – original draft, Writing – review & editing; **Jan Kielar:** Conceptualization, Data curation, Formal Analysis, Methodology, Software, Supervision, Validation

Data availability: All data required to repeat this research is provided in the text. Open-source codes to foster transparency and encourage reproducibility of this research are available under the CC BY 4.0 license at Zenodo; https://doi.org/10.5281/zenodo.17411891**.**

Electronic Appendices: All described files are given in Zenodo: https://doi.org/10.5281/zenodo.17367399

Electronic Appendix A: It includes an MS Excel tool that integrates key thermochemical processes of the Centre for Energy and Environmental Technologies – Explorer (CEETe, https://ceet.vsb.cz/en/CEETe/), which is used as a basis for https://shinyenet.vsb.cz/

Electronic Appendix B: It is given as an Excel table, which provides raw data sets from repeated gasification measurements. For example, for 750 °C gasification, results of four independent measurements are provided, in columns C, D, E, F. This article provides detailed regression analyses of the top six syngas components (O_2, CO_2, H_2, CO, CH_4, N_2), which cover approximately 98% of syngas, the line 'Sum of O_2, CO_2, H_2, CO, CH_4, N_2', i.e. B26 of the table. The absolute error of gasification measurements does not exceed 3.08 %, see the line 'Absolute error (0 % in theory)', the cell B28.

Electronic Appendix C: The Python file polynom.py is added to provide full reproducibility of results, which are related to bio-wood waste from the Czech Republic. However, the Python file, thanks to its general regression approach, can be applied to various alternative fuels for various countries. The Python file provides automated regression analyses and is accessible in the open repository, which automatically generates MS Word reports with color plots and tables given as a separate Word file. The Python file and the regression report provide a detailed analysis of the important syngas components (CO_2, H_2, CO, CH_4, and N_2) for regression models of degree 2 to 6, where the total of 5 times 5, i.e. 25, regression models are constructed and analyzed. The performance of these models is analyzed by various statistical metrics: max. absolute error, max. percentage error and mean squared error (MSE). Finally, the Python code and report include the most valuable regression models according to MSE. Interestingly, automated regression results clearly show that the winning (recommended) regression model for all analyzed syngas components is always represented by a polynomial of degree 4. In contrast to symbolic regression, which provides the overfitted models with artificial oscillations and non-physical peaks, classical regression models are very useful for modeling, Figures 9-13. Moreover, it can be seen that MSE is very close to zero and did not exceed 1.09, as can be seen in the Table on Page 6 of the file. Finally, each gas is tested using 5-fold cross-validation, see the Python file polynom_cross_validation.py.

 doi:10.20944/preprints202512.1609.v1

Degree 4 polynomials generally offer the best trade-off between bias and variance for most gases, except for N_2, where degree 2 polynomials generalize slightly better: The average MSE for the degree 2 polynomial is 0.8335, whereas for the degree 4 polynomial it is 0.965.

Declaration of conflicting interests: The authors declared no potential conflicts of interest with respect to the research, authorship, and/or publication of this article.

Funding: The authors received support from: 1. the Ministry of Education, Youth and Sports of the Czech Republic through the e–INFRA CZ (ID: 90254) project, 2. the EU funds under the project "Increasing the resilience of power grids in the context of decarbonisation, decentralisation and sustainable socioeconomic development", CZ.02.01.01/00/23_021/0008759, through the Operational Programme Johannes Amos Comenius, and 3. the Technology Agency of the Czech Republic through the CEET project—"Center of Energy and Environmental Technologies" TK03020027. Dejan Brkić additionally wants to acknowledge: This work has been supported by the Ministry of Science, Technological Development and Innovation of the Republic of Serbia, grant number: 451-03-136/2025-03/200102.

Declaration of generative AI in scientific writing: Not used.

Nomenclature (main text)

T - middle plasma torch temperature [K],

P - power of plasma torch [kW],

k - base constant of nozzle [dimensionless],

f_p - filling pressure [bar],

t - middle temperature in the gasification reactor [°C],

p - energy consumed in pyrolysis [MJ].

V – volume [m^3],

$G_{\%mass}$ - mass percentage of gas [%],

$L_{\%mass}$ - mass percentage of liquid fuel (pyrolysis oil) [%].

References

1. [1] Aich W, Hammoodi KA, Mostafa L, Saraswat M, Shawabkeh A, Said LB, El-Shafay AS, Mahdavi A. Techno-economic and life cycle analysis of two different hydrogen production processes from excavated waste under plasma gasification. Process Safety and Environmental Protection 2024; 184:1158-1176. https://doi.org/10.1016/j.psep.2024.02.055
2. [2] Awodun K, He Y, Wu C, Soltani SM. Catalytic pyrolysis of bio-waste in synthesis of value-added products: A systematic review. Fuel Processing Technology 2025;275:108258. https://doi.org/10.1016/j.fuproc.2025.108258
3. [3] Freda C, Giuliano A, Villone A, Cornacchia G, Catizzone E. Valorization of municipal solid waste from Marocco towards hydrogen, methanol, or electricity: An experimental and process simulation study. Fuel Processing Technology 2025; 275:108259. https://doi.org/10.1016/j.fuproc.2025.108259

 doi:10.20944/preprints202512.1609.v1

4. [5] Rizqi ZU. A simulation-based optimization approach for sustainable energy supply chain transitions. Supply Chain Analytics 2025; 27:100150. https://doi.org/10.1016/j.sca.2025.100150 [4] Aziz M, Darmawan A, Juangsa FB. Hydrogen production from biomasses and wastes: A technological review. International Journal of Hydrogen Energy 2021;46(68):33756-81. https://doi.org/10.1016/j.ijhydene.2021.07.189
5. [6] dos Santos RM, Szklo A, Lucena AFP, de Miranda PEV. Blue sky mining: Strategy for a feasible transition in emerging countries from natural gas to hydrogen. International Journal of Hydrogen Energy 2021; 46(51):25843-25859. https://doi.org/10.1016/j.ijhydene.2021.05.112
6. [7] Thomas R. The development of the manufactured gas industry in Europe. Geological Society, London, Special Publications 2018; 465(1):137-164. https://doi.org/10.1144/sp465.14
7. [8] Melaina MW. Market Transformation Lessons for Hydrogen from the Early History of the Manufactured Gas Industry. Chapter 5, In Hydrogen Energy and Vehicle Systems. CRC Press eBooks. 2012; 150-185. https://doi.org/10.1201/b13046-12
8. [9] Wehrer M, Rennert T, Mansfeldt T, Totsche KU. Contaminants at former manufactured gas plants: Sources, properties, and processes. Critical Reviews in Environmental Science and Technology 2011; 41(21):1883-1969. https://doi.org/10.1080/10643389.2010.481597
9. [10] Hamper MJ. Manufactured gas history and processes. Environmental Forensics 2006; 7(1):55-64. https://doi.org/10.1080/15275920500506790
10. [11] Albertazzi S, Basile F, Brandin J, Einvall J, Hulteberg C, Fornasari G, Rosetti V, Sanati M, Trifirò F, Vaccari A. The technical feasibility of biomass gasification for hydrogen production. Catalysis Today 2005; 106(1-4):297-300. https://doi.org/10.1016/j.cattod.2005.07.160
11. [12] Liebs, L.H. 1985. Town gas: An overview. AGA distribution/transmission conference. Boston, Massachusetts. Available from: https://semspub.epa.gov/work/01/458914.pdf (accessed on 22 May, 2024)
12. [13] Maksimov AL, Ishkov AG, Pimenov AA, Romanov KV, Mikhailov AM, Koloshkin EA. Physico-chemical aspects and carbon footprint of hydrogen production from water and hydrocarbons. Journal of Mining Institute 2024; 265:87-94. Available from: https://pmi.spmi.ru/pmi/article/view/16363/16227 (accessed on 21 June, 2024)
13. [14] Lyu H, He Y, Tang J, Hecker M, Liu Q, Jones PD, Codling G, Giesy JP. Effect of pyrolysis temperature on potential toxicity of biochar if applied to the environment. Environmental Pollution 2016; 218:1-7. https://doi.org/10.1016/j.envpol.2016.08.014
14. [15] Rutkowski JV, Levin BC. Acrylonitrile-butadiene-styrene copolymers (ABS): Pyrolysis and combustion products and their toxicity? A review of the literature. Fire and Materials 1986; 10(3-4):93-105. https://doi.org/10.1002/fam.810100303
15. [16] Rahimpour MR, Makarem MA, Meshksar M. eds., 2022. Advances in Synthesis Gas: Methods, Technologies and Applications. Elsevier eBooks. https://doi.org/10.1016/c2021-0-00292-3
16. [17] Odell WW. Facts Relating to the Production and Substitution of Manufactured Gas for Natural Gas. Department of Commerce, Bureau of Mines; 1929. Available from: https://books.google.rs/books?id=st4RRgrGA3sC&lr&pg (accessed on 21 June, 2024)
17. [18] Erdener BC, Sergi B, Guerra OJ, Chueca AL, Pambour K, Brancucci C, Hodge BM. A review of technical and regulatory limits for hydrogen blending in natural gas pipelines. International Journal of Hydrogen Energy 2023; 48(14):5595-5617. https://doi.org/10.1016/j.ijhydene.2022.10.254
18. [19] Ozturk M, Sorgulu F, Javani N, Dincer I. An experimental study on the environmental impact of hydrogen and natural gas blend burning. Chemosphere 2023; 329:138671. https://doi.org/10.1016/j.chemosphere.2023.138671
19. [20] Ascher S, Wang X, Watson I, Sloan W, You S. Interpretable machine learning to model biomass and waste gasification. Bioresource Technology 2022; 364:128062. https://doi.org/10.1016/j.biortech.2022.128062
20. [21] Li J, Li L, Tong YW, Wang X. Understanding and optimizing the gasification of biomass waste with machine learning. Green Chemical Engineering 2023; 4(1):123-133. https://doi.org/10.1016/j.gce.2022.05.006
21. [22] Lee J, Hong S, Cho H, Lyu B, Kim M, Kim J, Moon I. Machine learning-based energy optimization for on-site SMR hydrogen production. Energy Conversion and Management 2021; 244:114438. https://doi.org/10.1016/j.enconman.2021.114438

 doi:10.20944/preprints202512.1609.v1

22. [23] Chu C, Boré A, Liu XW, Cui JC, Wang P, Liu X, Chen GY, Liu B, Ma WC, Lou ZY, Tao Y. Modeling the impact of some independent parameters on the syngas characteristics during plasma gasification of municipal solid waste using artificial neural network and stepwise linear regression methods. Renewable and Sustainable Energy Reviews 2022; 157:112052. https://doi.org/10.1016/j.rser.2021.112052
23. [24] Kaheel S, Ibrahim KA, Fallatah G, Lakshminarayanan V, Luk P, Luo Z. Advancing Hydrogen: A Closer Look at Implementation Factors, Current Status and Future Potential. Energies 2023; 16(24):7975. https://doi.org/10.3390/en16247975
24. [25] Hasanzadeh R, Mojaver P, Azdast T, Chitsaz A, Park CB. Low-emission and energetically efficient co-gasification of coal by incorporating plastic waste: a modeling study. Chemosphere 2022;299:134408. https://doi.org/10.1016/j.chemosphere.2022.134408
25. [26] Raj R, Singh DK, Tirkey JV. Co-gasification of plastic waste blended with coal and biomass: A comprehensive review. Environmental Technology Reviews 2023;12(1):614-42. https://doi.org/10.1080/21622515.2023.2283095
26. [27] Smoliński A, Howaniec N, Gąsior R, Polański J, Magdziarczyk M. Hydrogen rich gas production through co-gasification of low rank coal, flotation concentrates and municipal refuse derived fuel. Energy 2021;235:121348. https://doi.org/10.1016/j.energy.2021.121348
27. [28] Zainal BS, Ker PJ, Mohamed H, Ong HC, Fattah IM, Rahman SA, Nghiem LD, Mahlia TI. Recent advancement and assessment of green hydrogen production technologies. Renewable and Sustainable Energy Reviews 2024; 189:113941. https://doi.org/10.1016/j.rser.2023.113941
28. [29] Oh S, Park SR, Kang YT. Optimum design of high-temperature steam generator for hydrogen production enhancement. International Journal of Energy Research 2023; 2023(1):9022385. https://doi.org/10.1155/2023/9022385
29. [30] Chojnacki J, Kielar J, Kukiełka L, Najser T, Pachuta A, Berner B, Zdanowicz A, Frantík J, Najser J, Peer V. Batch pyrolysis and co-pyrolysis of beet pulp and wheat straw. Materials 2022; 15(3):1230. https://doi.org/10.3390/ma15031230
30. [31] Chojnacki J, Kielar J, Najser J, Frantík J, Najser T, Mikeska M, Gaze B, Knutel B. Straw pyrolysis for use in electricity storage installations. Heliyon 2024: 10(9):e30058. https://doi.org/10.1016/j.heliyon.2024.e30058
31. [32] Čespiva JA, Wnukowski M, Skřínský J, Perestrelo R, Jadlovec M, Výtisk J, Trojek M, Câmara JS. Production efficiency and safety assessment of the solid waste-derived liquid hydrocarbons. Environmental Research 2024; 244:117915. https://doi.org/10.1016/j.envres.2023.117915
32. [33] Vaculik J, Hradilek Z, Moldrik P, Minarik D. Calculation of efficiency of hydrogen storage system at the fuel cells laboratory. In Proceedings of the 2014 15th International Scientific Conference on Electric Power Engineering (EPE) (pp. 381-384). IEEE. https://doi.org/10.1109/epe.2014.6839440
33. [34] Najser J, Frantik J. Smart Grid System Using Electricity from Photovoltaics, Renewable Sources and Alternative Fuels. Proceedings of the ISES Solar World Congress 2019. https://doi.org/10.18086/swc.2019.19.07
34. [35] Hlaba A, Rabiu A, Osibote OA. Thermochemical Conversion of Municipal Solid Waste — An Energy Potential and Thermal Degradation Behavior Study. International Journal of Environmental Science and Development 2016, 7(9):661-667. https://doi.org/10.18178/ijesd.2016.7.9.858
35. [36] Pacheco N, Ribeiro A, Oliveira F, Pereira F, Marques L, Teixeira JC, Vilarinho C, Barbosa FV. Sewage sludge plasma gasification: Characterization and experimental rig design. Reactions 2024; 5(2):285-304. https://doi.org/10.3390/reactions5020014
36. [37] Kongprawes G, Wongsawaeng D, Hosemann P, Ngaosuwan K, Kiatkittipong W, Assabumrungrat S. Dielectric barrier discharge plasma for catalytic-free palm oil hydrogenation using glycerol as hydrogen donor for further production of hydrogenated fatty acid methyl ester (H-FAME). Journal of Cleaner Production 2023; 401:136724. https://doi.org/10.1016/j.jclepro.2023.136724
37. [38] Sarantaridis D, Fowowe T, Caruana DJ. Electrochemistry in flames. Science Progress 2010; 93(3):301-317. https://doi.org/10.3184/003685010X12710040579074
38. [39] Elaissi S, Alsaif NAM. Modeling and Performance Analysis of municipal solid waste treatment in plasma torch reactor. Symmetry 2023; 15(3):692. https://doi.org/10.3390/sym15030692

 doi:10.20944/preprints202512.1609.v1

39. [40] Leal-Quirós E. Plasma processing of municipal solid waste. Brazilian Journal of Physics 2004; 34(4b):1587-1593. https://doi.org/10.1590/s0103-97332004000800015
40. [41] Dubčáková R. Eureqa: software review. Genetic Programming and Evolvable Machines 2010; 12(2):173-178. https://doi.org/10.1007/s10710-010-9124-z
41. [42] Brkić D, Praks P, Marek M, Ilić U, Stajić Z. Reducing the number of input variables through symbolic regression. Electronic Research Archive 2025;33(9):5158-78. https://doi.org/10.3934/era.2025231
42. [43] Hasanzadeh R, Mojaver M, Azdast T, Park CB. A novel systematic multi-objective optimization to achieve high-efficiency and low-emission waste polymeric foam gasification using response surface methodology and TOPSIS method. Chemical Engineering Journal 2022;430:132958. https://doi.org/10.1016/j.cej.2021.132958
43. [44] Čespiva J, Skřínský J, Vereš J, Borovec K, Wnukowski M. Solid-recovered fuel to liquid conversion using fixed bed gasification technology and a Fischer–Tropsch synthesis unit – case study. International Journal of Energy Production and Management 2020; 5(3):212-222. https://doi.org/10.2495/eq-v5-n3-212-222
44. [45] Becker WL, Braun RJ, Penev M, Melaina M. Production of Fischer–Tropsch liquid fuels from high temperature solid oxide co-electrolysis units. Energy 2012; 47(1):99-115. https://doi.org/10.1016/j.energy.2012.08.047
45. [46] Zhang K, Harvey AP. CO_2 decomposition to CO in the presence of up to 50% O_2 using a non-thermal plasma at atmospheric temperature and pressure. Chemical Engineering Journal 2021; 405:126625. https://doi.org/10.1016/j.cej.2020.126625
46. [47] Praks P, Lampart M, Praksová R, Brkić D, Kozubek T, Najser J. Selection of appropriate symbolic regression models using statistical and dynamic system criteria: example of waste gasification. Axioms 2022; 11(9):463-463. https://doi.org/10.3390/axioms11090463
47. [48] Chang P-Y, Yang P-Y, Chou F-I, Chen S-H. Hybrid optimization algorithm for thermal displacement compensation of computer numerical control machine tool using regression analysis and fuzzy inference. Science Progress 2023; 106(2). https://doi.org/10.1177/00368504231171268
48. [49] Udrescu SM, Tegmark, M. (2020). AI Feynman: A physics-inspired method for symbolic regression, Science Advances 2020; 6(16). https://doi.org/10.1126/sciadv.aay2631
49. [50] Praks P, Brkić D, Najser J, Najser T, Praksová R, Stajić Z. Methods of Artificial Intelligence for Simulation of Gasification of Biomass and Communal Waste, 2021 22nd International Carpathian Control Conference (ICCC), Velké Karlovice, Czech Republic, 2021, https://doi.org/10.1109/iccc51557.2021.9454641
50. [51] Cranmer M, Interpretable Machine Learning for Science with PySR and SymbolicRegression.jl, 2023, https://doi.org/10.48550/arXiv.2305.01582
51. [52] Smith WR, Tahir H, Leal AMM. Stoichiometric and non-stoichiometric methods for modeling gasification and other reaction equilibria: A review of their foundations and their interconvertibility. Renewable and Sustainable Energy Reviews 2024; 189:113935-113935. https://doi.org/10.1016/j.rser.2023.113935
52. [53] Dell RM, Moseley PT, Rand DAJ. Chapter 8 - Hydrogen, Fuel Cells and Fuel Cell Vehicles. In Towards Sustainable Road Transport 2014; 260-295. https://doi.org/10.1016/b978-0-12-404616-0.00008-6
53. [54] Mekhilef S, Saidur R, Safari A. Comparative study of different fuel cell technologies. Renewable and Sustainable Energy Reviews 2012; 16(1):981-989. https://doi.org/10.1016/j.rser.2011.09.020
54. [55] Wu C, Zhu Q, Dou B, Fu Z, Wang J, Mao S. Thermodynamic analysis of a solid oxide electrolysis cell system in thermoneutral mode integrated with industrial waste heat for hydrogen production. Energy 2024; 301:131678. https://doi.org/10.1016/j.energy.2024.131678
55. [56] Martinez Lopez VA, Ziar H, Haverkort JW, Zeman M, Isabella O. Dynamic operation of water electrolyzers: A review for applications in photovoltaic systems integration. Renewable and Sustainable Energy Reviews 2023; 182:113407. https://doi.org/10.1016/j.rser.2023.113407
56. [57] Perry RH, Green DW. Perry's chemical engineers' handbook. 8th ed. New York: McGraw-Hill, 2008, ISBN 9780071422949
57. [58] Krylova AY, Products of the Fischer-Tropsch synthesis (A Review). Solid Fuel Chem, 2014, 48, 22–35, https://doi.org/10.3103/S0361521914010030

 doi:10.20944/preprints202512.1609.v1

58. Konstandopoulos AG, Syrigou M, Pagkoura C, Sakellariou K, Lorentzou S, et al. Solar fuels and industrial solar chemistry. Concentrating Solar Power Technology, Elsevier, 2021, 677-724. https://doi.org/10.1016/B978-0-12-819970-1.00005-0
59. Chakraborty JP, Singh S, a Maity SK. Advances in the conversion of methanol to gasoline. Hydrocarbon Biorefinery, Elsevier, 2022, 177-200. https://doi.org/10.1016/B978-0-12-823306-1.00008-X
60. Kalkreuth W, Ruaro Peralba M, Barrionuevo S, Hinrichs R, Silva T, Maman Anzolin H, Osório E, Pohlmann J, De Caumia B, Pakdel H, Roy C. Vacuum Pyrolysis of Brazilian coal, peat and biomass–Results on characterization of feedstock, solid residues, pyrolysis liquids and conversion rates. Energy Exploration & Exploitation 2024; 42(3):817-836. https://doi.org/10.1177/01445987231225253
61. Du Y, Ju T, Meng Y, Han S, Jiang J. Pyrolysis characteristics of excavated waste and generation mechanism of gas products. Journal of Cleaner Production 2022; 370:133489-133489. https://doi.org/10.1016/j.jclepro.2022.133489
62. Çelik A, Othman IB, Müller H, Lott P, Deutschmann O. Pyrolysis of biogas for carbon capture and carbon dioxide-free production of hydrogen. Reaction Chemistry & Engineering 2024; 9(1):108-118. https://doi.org/10.1039/D3RE00360D
63. Aldeia GSI, de França FO. Interpretability in symbolic regression: a benchmark of explanatory methods using the Feynman data set. Genetic Programming and Evolvable Machines 2022; 23:309-349. https://doi.org/10.1007/s10710-022-09435-x
64. Praks P, Rasmussen A, Lye KO, Martinovič J, Praksová R, Watson F, Brkić D. Sensitivity analysis of parameters for carbon sequestration: Symbolic regression models based on open porous media reservoir simulators predictions. Heliyon 2024; 10(22): e40044. https://doi.org/10.1016/j.heliyon.2024.e40044
65. Staš M, Auersvald M, Kejla L, Vrtiška D, Kroufek J, Kubička D. Quantitative analysis of pyrolysis bio-oils: A review. TrAC Trends in Analytical Chemistry 2020;126:115857. https://doi.org/10.1016/j.trac.2020.115857
66. Xin Q, Farooqi H, Lang J, Al-Haj B, Saborimanesh N. Behavioral and toxicological impacts of bio-derived oils in aqueous spills. Journal of Environmental Chemical Engineering 2024;12(6):114353. https://doi.org/10.1016/j.jece.2024.114353
67. Chatterjee N, Eom HJ, Jung SH, Kim JS, Choi J. Toxic potentiality of bio-oils, from biomass pyrolysis, in cultured cells and Caenorhabditis elegans. Environmental Toxicology 2014;29(12):1409-19. https://doi.org/10.1002/tox.21871
68. Chai CH, Chan CY, Heng JZ, Tang KY, Loh XJ, Li Z, Ye E. Converting plastic waste to fuel and fine chemicals. InCircularity of Plastics 2023 Jan 1 (pp. 71-100). Elsevier. https://doi.org/10.1016/B978-0-323-91198-6.00001-2
69. Flood MW, EntropyHub, https://www.entropyhub.xyz/
70. Buchlovská Nagyová J, Jansík B, Lampart M. Detection of embedded dynamics in the Györgyi-Field model. Scientific Reports 2020; 10:21031, https://doi.org/10.1038/s41598-020-77874-6
71. Lampart M, Vantuch T, Zelinka I, Mišák S. Dynamical properties of partial-discharge patterns. International Journal of Parallel, Emergent and Distributed Systems 2018; 33(5):474–489, https://doi.org/10.1080/17445760.2017.1324026
72. Lampart M, Zapoměl J. Motion of an unbalanced impact body colliding with a moving belt. Mathematics 2021; 9(9):1071. https://doi.org/10.3390/math9091071.